https://doi.org/10.5194/essd-2020-68
Preprint. Discussion started: 6 April 2020

Open Access Earth System Science Data Discussions

Global anthropogenic CO_2 emissions and uncertainties as prior for Earth system modelling and data assimilation

Margarita Choulga[1], Greet Janssens-Maenhout[2], Ingrid Super[3], Anna Agusti-Panareda[1], Gianpaolo Balsamo[1], Nicolas Bousserez[1], Monica Crippa[2], Hugo Denier van der Gon[3], Richard Engelen[1], Diego Guizzardi[2], Jeroen Kuenen[3], Joe McNorton[1], Gabriel Oreggioni[2], Efisio Solazzo[2], and Antoon Visschedijk[3]

[1]Research Department, ECMWF, Reading, RG2 9AX, United Kingdom
[2]Joint Research Centre of the European Commission, EC-JRC, Ispra, 21027, Italy
[3]TNO, Department of Climate, Air and Sustainability, Utrecht, 3584 CB, The Netherlands

Correspondence to: Margarita Choulga (margarita.choulga@ecmwf.int)

Abstract. Anthropogenic carbon dioxide (CO_2) emissions and their observed growing trends raise awareness in scientific, political and public sectors of the society as the major driver of climate-change. For an increased understanding of the CO_2 emission sources, patterns and trends, a link between the emission inventories and observed CO_2 concentrations is best established via Earth system modelling and data assimilation. In this study anthropogenic CO_2 emission inventories are processed into gridded maps to provide an estimate of prior CO_2 emissions for 7 main emissions groups: 1) power generation super-emitters and 2) energy production average-emitters, 3) manufacturing, 4) settlements, 5) aviation, 6) transport and 7) others, with estimation of their uncertainty and covariance to be included in the European Centre for Medium-Range Weather Forecasts (ECMWF) Integrated Forecasting System (IFS). The emission inventories are sourced from the Intergovernmental Panel on Climate Change (IPCC) 2006 Guidelines for National Greenhouse Gas Inventories and revised information from its 2019 Refinements, and the global grid-maps of Emissions Database for Global Atmospheric Research (EDGAR) inventory. The anthropogenic CO_2 emissions for 2012 and 2015, (EDGAR versions 4.3.2 and 4.3.2_FT2015 respectively) are considered, updated with improved apportionment of the energy sector, energy usage for manufacturing and diffusive CO_2 emissions from coal mines. These emissions aggregated into 7 ECMWF groups with their emission uncertainties are calculated per country considering its statistical infrastructure development level and sector considering the most typical fuel type and use the IPCC recommended error propagation method assuming fully uncorrelated emissions to generate covariance matrices of parsimonious dimension (7×7). While the uncertainty of most groups remains relatively small, the largest contribution to the total uncertainty is determined by the group with usually the smallest budget, consisting of oil refineries and transformation industry, fuel exploitation, coal production, agricultural soils and solvents and products use emissions. Several sensitivity studies are performed: for country type (with well-/less well-developed statistical infrastructure), for fuel type specification, and for national emission source distribution (highlights the importance of accurate point source mapping). Uncertainties are compared with United Nations Framework Convention on Climate Change (UNFCCC) and the Netherlands Organisation for Applied Scientific Research (TNO) data. Upgraded anthropogenic

https://doi.org/10.5194/essd-2020-68
Preprint. Discussion started: 6 April 2020

Open Access Earth System Science Data Discussions

CO_2 emission maps with their yearly and monthly uncertainties are combined into the CHE_EDGAR-ECMWF_2015 dataset (Choulga et al., 2020) available from doi:10.5281/zenodo.3712339.

1 Introduction

Carbon dioxide (CO_2) is the most abundant greenhouse gas (GHG) (NOAA, 2019) contributing to the Earth's radiative balance and climate stability. This study focuses on anthropogenic (man-made) long carbon cycle (period between carbon release to and capture from the atmosphere is longer than a year) CO_2 emissions, that occur on top of an active natural carbon cycle, and generation of a reliable uncertainty band globally for different emission types that can be used in Earth system modelling and data assimilation.

The CO_2 growth rate varies from year to year with a tendency toward higher growth rates since the early 2002s. The added CO_2 has a long life-time and only a portion of it transfers each year from the atmosphere to the oceans and to vegetation on land. The atmosphere exchanges carbon mainly between: (i) the terrestrial biosphere – is influenced through deforestation and other forms of land management; (ii) the oceans – marine ecosystems have implications due to CO_2 in the form of carbonic acid absorption in surface waters and their mix with deep ocean waters; (iii) the fossil fuels and cement and other CO_2 process emissions – around 1920 fossil fuel burning became the dominant source of anthropogenic emissions to the atmosphere and there is a clear increase of 91 ppm since 1959 (316 ppm) till 2018 (407.4 ± 0.1 ppm), according to NOAA (2019).

Accurate assessment of anthropogenic CO_2 emissions is important to better understand the global carbon cycle. Efforts towards a global anthropogenic CO_2 monitoring and verification support capacity as described by Janssens-Maenhout et al. (2020), rely on atmospheric modelling and atmospheric observations (in-situ from e.g. the Integrated Carbon Observatory System, air-borne from e.g. aircraft campaigns, or space-borne from e.g. the Orbiting Carbon Observatory, OCO-2, and the Greenhouse gases Observing Satellite, GOSAT). All measurements are assimilated by global tracer transport models to infer atmospheric CO_2 changes or by flux inversion systems to estimate the large-scale surface CO_2 fluxes. ECMWF applies both inverse modelling and direct modelling of global concentrations of CO_2 in the atmosphere assimilating several types of observations.

The global transport models require an initial best estimate of the CO_2 emission fields with uncertainties, the so-called prior information. The intensity of the emission fields is corrected through minimization of the difference between the modelled and measured concentration values for CO_2. The uncertainty of these corrected CO_2 fluxes based on inverse modelling will be lower with the increase of CO_2 observations and its accuracy. The disentanglement of the fossil CO_2 emissions from the total atmospheric CO_2 concentration remains challenging, e.g. in 2018 total anthropogenic CO_2 concentrations (42.5 ± 3.3 Gt CO_2) represented only 1.3 % of the global atmospheric CO_2 concentration (407.4 ± 0.1 ppm) (Friedlingstein et al., 2019; Mitchell, 1984), which states the need for high accuracy of measurements (≥ 1.0 %).

https://doi.org/10.5194/essd-2020-68
Preprint. Discussion started: 6 April 2020

Global tracer transport models also require input of emission data, which is often supplied through emission inventories. Bottom-up emission inventories start from human activity statistics and emission factors (EF) are defined for each activity and provided at international or country level (e.g. National greenhouse gas Inventory Report, NIR). Such bottom-up inventories need to be gridded and characterised with uncertainties in order to represent a prior data set useful for numerical modelling. Table 1 shows some examples of global gridded CO_2 emission datasets, for more details see Andrew (2020), Janssens-Maenhout et al. (2019, Table 3) and Cong et al. (2018, Table 1).

Table 1: Some examples of global gridded CO_2 emission datasets

Name	Resolution	Period	Note	Source
Carbon Dioxide Information Analysis Center (CDIAC)	Spatial: 1.0°×1.0° Temporal: annual, monthly	1751-2013	Use population density to disaggregate emissions, the mass-emissions data based on fossil-fuel consumption estimates. Provide gridded annual and monthly uncertainty estimates for 1950-2013	Andres et al., 1996; Andres et al., 2016
Open-Data Inventory for Anthropogenic Carbon dioxide (ODIAC)	Spatial: 1×1 km^2, 0.1°×0.1° Temporal: monthly	1979-2018	First introduced the combined use of nightlight data and individual power plant emission/location profiles	Oda and Maksyutov, 2011; ODIAC, 2020
Emissions Database for Global Atmospheric Research (EDGAR)	Spatial: 0.1°×0.1° Temporal: annual, monthly	1970-(year-1)	Based on international statistics, covers all IPCC (2006) reporting categories, consistent methodology applied to all the world countries	Janssens-Maenhout et al., 2019
Fossil Fuel Data Assimilation System (FFDAS)	Spatial: 0.1°×0.1° Temporal: annual	1997-2012	Provide gridded posterior uncertainty (version 2.2); in addition, provide monthly, weekly, and hourly fractions from annual CO_2 emissions	Asefi-Najafabady et al., 2014
Community Emissions Data System (CEDS)	Spatial: 0.1°×0.1° Temporal: annual, monthly	1750-2014	Provide emissions of CO_2 and other GHGs and pollutants	Hoesly et al., 2018
Peking University Fuel combustion inventory (PKU-FUEL)	Spatial: 0.1°×0.1° Temporal: monthly	1960-2014	By request provide daily emissions and the results of Monte Carlo simulation-based uncertainty analyses	Chen et al., 2016; Liu et al., 2015

Global emission budget values from different datasets are never the same, therefore it is important to identify why estimates differ between datasets (e.g. differences in sources and methods used or emission double counting and omissions). Though there are global anthropogenic emission gridded datasets, most of them have scarce evaluation of uncertainties, which needs enhancement with the relative errors for sector-specific country totals and the uncertainties in trends with the appropriate probability density functions. Global gridded uncertainties used in an independent atmospheric inversion method might also increase level of confidence in a certain emission dataset (Andrew, 2020).

In this study, we focus on fossil emissions (from fossil fuel combustion, use and production, and process emissions from cement production and others such as glass, chemicals, urea) with long carbon cycle and we distinguish between point sources and sources with wider spatial distribution. The scope of this research is to generate a reliable uncertainty band with global coverage based on emission type for the yearly and monthly emission budgets, that are the composite of anthropogenic fossil fluxes. Uncertainty characterisation is key for optimally combining the bottom-up inventories with the top-down data assimilation.

https://doi.org/10.5194/essd-2020-68
Preprint. Discussion started: 6 April 2020

Open Access Earth System Science Data Discussions

In this study 2015 is chosen as a base year to analyse anthropogenic CO_2 budgets (i.e. global, regional, national) from different sources (i.e. global statistics, national reports). Main reason for this choice is the presence of observations (both in-situ and space-borne), and that all available information is already verified and reported. Global CO_2 emissions from fossil fuel and industrial processes such as cement production reached a total of 36.2 Pg CO_2 in 2015 according to EDGAR inventory version 4.3.2_FT2015 (Olivier et al., 2016a). This result shows a stagnation of the fossil emissions growth, also thanks to the curbing of China's emissions. Largest contribution to this global total originates from China (with a 29 % share in the global total), the United States (14 %), the European Union (28 members till end of 2019) (10 %), India (7 %), the Russian Federation (5 %). The use of energy represents by far the largest source of emissions (89 % share globally). The energy industry sector includes emissions from fuel combustion (the large majority, with 38 % share) and fugitive emissions, which are intentional or unintentional releases of gas from production, processes, transmission, storage and use of fuels. Other sectors manufacturing, transport and buildings show a share of 22 %, 20 % and 9 % respectively in 2015. More details are given in Olivier et al. (2016b). Another reason for choosing 2015 is that it's the year of the Paris Agreement and the reference year for several Nationally Determined Contributions (NDCs) (most countries in their NDCs also mention years 1990, 2005, 2025 and 2030). On 12th December 2015 at the twenty-first session of the Conference of the Parties to the United Nations Framework Convention on Climate Change the Paris Agreement was agreed, and currently it is ratified by 189 countries (CarbonBrief, 2020; Paris Agreement - Status of Ratification, 2020). It aims to limit the increase in global average temperature to 1.5 ºC, since this would significantly reduce risks and the impacts of climate change (Paris Agreement, 2020). Countries have submitted their pledges to the United Nations (UN), setting out how far they plan to reduce their GHG emissions – NDCs (CarbonBrief, 2020). For example, the European Union's NDC under the Paris Agreement is to reduce GHG emissions by at least 40 % by 2030 compared to 1990 (Paris Agreement, 2020). Yet concentrations are still growing. In 2015, the average concentration of CO_2 (399 ppm) was about 40 % higher than in the mid-1800s, with an average growth of 2 ppm/yr in the last ten years. CO_2 resulting from the oxidation of carbon in fuels during combustion dominates total GHG emissions. Furthermore, according to JRC 2019 Report (Crippa et al., 2019) between 2015 till 2018, just in three years global CO_2 emissions have raised by 4.3 % (1575.2 Mt CO_2/yr), while international shipping and aviation CO_2 emissions have raised by 6.1 % and 6.6 % (40.2 and 34.9 Mt CO_2/yr) respectively.

Following the Intergovernmental Panel on Climate Change (IPCC) 2006 Guidelines for National Greenhouse Gas Inventories and revised information from its 2019 Refinements (IPCC-TFI, 2019) we start from the global fossil CO_2 grid-maps of EDGAR inventory versions 4.3.2 (Janssens-Maenhout et al., 2019) and 4.3.2_FT2015 (Olivier et al., 2016a), for 2012 and 2015 respectively, and derive an updated emission dataset as prior input to the ECMWF model: CHE_EDGAR-ECMWF_2015 (CHE stands for the CO_2 Human Emissions project (CHE, 2020)). We improve the apportionment of the energy sector and the energy used for manufacturing, add the diffusive CO_2 emissions from coal mines and aggregate the sectors in 7 emission groups while tracking 232 countries separately. Uncertainties are calculated per country and sector considering the most typical fuel type using the error propagation method of the IPCC (2006) guidelines. According to the IPCC (2006) guidance all emissions are considered to be fully uncorrelated; this assumption is further used to calculate

https://doi.org/10.5194/essd-2020-68
Preprint. Discussion started: 6 April 2020

Open Access Earth System Science Data Discussions

uncertainty and covariance matrices. The country-based uncertainties and the share to the total uncertainty are presented for the 7 ECMWF emission groups, with calculations based on 20 EDGAR sectors for two distinct country types with well- and less well-developed statistical infrastructure. While the uncertainty of most groups (i.e. power industry, combustion for manufacturing, and road transport) remains small, the largest contribution to the total uncertainty is determined by rather small but relative uncertain sectors (i.e. non energy use of fuels, chemical processes, fuel exploitation, and coal production) emissions.

This paper is organised as follows. Section 2 describes the data sources and includes the description of the anthropogenic CO_2 emission datasets used to calculate emission uncertainties, data pre-processing, emission sectors and groups, and geographical treatment of emissions. Section 3 discusses the uncertainty calculation methodology applied to the datasets, to calculate both yearly and monthly uncertainties. Emission country and sector budgets comparison with other institute data and discussion of the results and further developments are covered in Section 4 dedicated to comparison and discussion. The main results, a discussion and further research guidance are covered in the conclusion in Section 5. This paper also has Supplementary Information with details on methods and assumptions used.

2 Data

2.1 Update of fossil CO_2 emissions as input for the ECMWF model

Main requirements for datasets in order to be used in global numerical models are being global and gridded, and preferably with continuous update. In this study it was decided to use EDGARv4.3.2 (and EDGARv4.3.2_FT2015) because it is based on international statistics, mainly International Energy Agency (IEA) data, has a unique global geo-coverage with 228 countries/regions and continuous updates with time-series from 1970 onwards, till the year-1. EDGAR distributes anthropogenic emissions for each source category over a uniform, global 0.1°×0.1° grid defined with lower left coordinates and provides annual and monthly global emissions grid-maps. In emission inventories the emissions can be emitted either from a single point source (e.g. power plants, factories) or distributed over a linear source (e.g. roads) or over an area source (e.g. agricultural fields), depending on the source sector or subsector. The bottom-up emissions calculation methodology and (mainly default) EFs are consistently applied to all countries in order to achieve comparability and full transparency. Region-specific EFs are selected, when these are recommended by IPCC (2006) guidelines or when these are justified by robust information on significant differences in economic activities, in customs or in geographical ambient conditions and proven to be more representative than the global average. All sectors based on fuel or product consumption statistics are considered. We focus on long carbon cycle CO_2 and therefore consider the CO_2 from fossil fuel use (combustion and other use) and from industrial processes (cement production, carbonate use of limestone and dolomite, non-energy use of fuels and other combustion, chemical and metal processes, solvents, agricultural liming and urea, waste and fossil fuel fires). Excluded are consumption of biofuels and short-cycle biomass burning (such as agricultural waste burning), large-scale biomass burning (such as forest fires, Savannah burning, woodland and peatland fires) and carbon emissions/removals of land-use, land-use

https://doi.org/10.5194/essd-2020-68
Preprint. Discussion started: 6 April 2020

change and forestry (LULUCF)[1]. Based on the Global Carbon Budget 2018 findings this sector showed no significant trend since 1960s, only high year-to-year variability and high uncertainty (Bastos et al., 2020; Le Quéré et al., 2018; Arneth et al., 2017). We excluded also the fossil fuel fires, because we do not focus on historical time series but on 2015 (so the Kuwait oil fires of 1991 are of no importance) and the coal mine fires data are considered to be very uncertain. The most relevant activity data (AD) for our CHE_EDGAR-ECMWF_2015 are the energy statistics from IEA (2014), which has been corrected for few outliers and for the revised Chinese coal statistics of 2015.

While EDGARv4.3.2 provides emissions of 150 activities, and 42 fossil fuels, there was a need to re-attribute part of the energy sector to the manufacturing industry in order to match the United Nations Framework Convention on Climate Change (UNFCCC) reporting. EDGARv4.3.2_FT2015 energy sector emissions were divided into autoproducers and the rest. The autoproducing energy part was added to the industry sector as it is generated purposely for manufacturing, and not for power generation in general. The autoproducers part reported in the energy statistics by every country separately (IEA, 2016) was reattributed to the manufacturing in CHE_EDGAR-ECMWF_2015 but the correction remained limited to 30 % of the total energy sector. More details are given in the Supplementary Information, section S.1.

Another update resulted in the expansion of the emissions with the fugitive CO_2 from coal mines, following the recommendations from IPCC-TFI (2019). Even though this emission source is not that large globally, it is a highly uncertain emission source that was detected by space-borne images over the United States of America. An additional map for CHE_EDGAR-ECMWF_2015 with coal mining emissions from underground mines has been generated, following the IPCC-TFI (2019) default values and the coal mining activity of the methane (CH_4) emission grid-maps from hard and brown coal production of EDGARv4.3.2. More details are given in the Supplementary Information, section S.2.

The detailed EDGARv4.3.2 spatial distribution is used for mapping the updated 2015 emission values. For the update from 2012 to 2015 we used the fast track approach of Olivier et al. (2016b), with IEA (2016) energy statistics and BP (2017) statistics. The relative changes per sector, fuel type and country from 2012 to 2015 are then applied on the EDGARv4.3.2 reference maps to obtain EDGARv4.3.2_FT2015.

For non-energy use of fuels, chemical processes, and solvents and products use we used directly the EDGARv4.3.2 maps. Also, the CO_2 emission maps from coal production are based on the 2012 maps of CH_4 from EDGARv4.3.2. Gridded monthly multiplication factors are obtained from 2010 monthly gridded emissions and applied to the final set of yearly emission maps of CHE_EDGAR-ECMWF_2015.

For the full list of differences between EDGARv4.3.2_FT2015 and CHE_EDGAR-ECMWF_2015, we refer to the Supplementary Information, section S.2 Table S3.

[1] Following the UNFCCC national inventory reporting guidelines, emissions of biofuel combustion are only a memo item and have to be reported under the LULUCF sector. Together with all short-cycle carbon emissions they are excluded from this study.

https://doi.org/10.5194/essd-2020-68
Preprint. Discussion started: 6 April 2020

Earth System Science Data
Open Access
Discussions

2.2 Aggregation of CO_2 emission groups for the ECMWF model

EDGARv4.3.2_FT2015 (as well as EDGARv4.3.2) has 20 global maps with anthropogenic long carbon cycle CO_2 flux values for energy, fugitives, industrial processes, solvents and products use, agriculture and waste involved sectors. In this study these sectors had to be grouped for the use of global flux inversion and ensemble perturbation systems. Grouping was done keeping in mind possible future evolution of present systems and sector common features: activity type (point sources, 3D field, etc.), amount of knowledge for the activity (uncertainty value), geographical distribution (e.g. over urban areas only), size of sector covariance matrix. An adequate size for the inversion system of the ECMWF model is less than 50 and a covariance matrix of 7×7 has been chosen. Table 2 shows additional grouping of 20 EDGAR sectors into 7 ECMWF groups. The remaining energy sector (after autoproducers part separation) was divided into one produced by super power plants, and one produced by average (non-super) power plants. As super power plants are considered grid-cells with annual flux $7.9 \cdot 10^{-6}$ $kg \cdot m^{-2} \cdot s^{-1}$ and higher. In total there are 30 super power plant grid-cells, all the remaining energy sector grid-cells are assumed to have emissions from the average power plants. For the detailed ranking of the power plant sites in function of their emission intensity, we refer to the Supplementary Information, section S.1.

3 Uncertainty calculation methodology

3.1 Overview

The IPCC (2006) Guidelines for NIR for fossil CO_2 uncertainty calculations and updated IPCC-TFI (2019) provide vast information about numerous human activities emitting CO_2 and how certain these values are. Use of the IPCC-TFI (2019) permitted to consider the 2019 EF and AD uncertainties for petroleum refining, solid fuel manufacturing, transformation, processing and transport and oil and gas production, which differed significantly from the 2006 defaults. In order to use the same methodology globally and because CO_2 emissions are not technologically dependant, it was decided to omit regional (e.g. Europe) detailed information and use only information required for the most basic and simplest (Tier 1) approach for emission reporting. The Tier 1 methodology to estimate CO_2 emissions from fossil fuel combustion follows the concept of carbon conservation (from the fuel combusted into CO_2). Uncertainties for all emission activities, sectors and groups can be derived following two different approaches of IPCC (2006): (Approach 1) propagation of error – gives informative results even if the criterion "standard deviation divided by the mean value is less than 0.3" is not strictly met and data still have some correlation. The advantages are that it only needs uncertainty ranges for AD and EF, that are provided by IPCC and that it is relatively easy to improve in case of large and asymmetric uncertainties; (Approach 2) Monte Carlo simulation or similar techniques – suitable only if detailed category-by-category uncertainty information is available and complex calculations can be done. In order to use the same methodology for all world countries/geographical entities (i.e. not needing detailed information for each emission activity) it was decided to use the error propagation method (Approach 1).

https://doi.org/10.5194/essd-2020-68
Preprint. Discussion started: 6 April 2020

Table 2: Additional grouping of anthropogenic long carbon cycle CO_2 emission EDGAR sectors (with global emission budgets for 2015 in Mton) into ECMWF groups

№	ECMWF group	IPCC (2006) activities per EDGAR sector	Note	Emission budget, Mton
1	ENERGY_S	1.A.1.a (subset)	Power industry (without autoproducers): super emitting power plants	896.7
2	ENERGY_A	1.A.1.a (rest)	Power industry (without autoproducers): average emitting power plants	11671.6
		4.C	Solid waste incineration	137.2
3	MANUFACTURING	1.A.2	Combustion for manufacturing (including autoproducers)	7320.4
		2.C.1, 2.C.2	Iron and steel production	233.6
		2.C.3, 2.C.4, 2.C.5, 2.C.6, 2.C.7	Non-ferrous metals production	91.4
		2.D.1, 2.D.2, 2.D.4	Non energy use of fuels	24.6
		2.A.1, 2.A.2, 2.A.3, 2.A.4	Non-metallic minerals production	1749.0
		2.B.1, 2.B.2, 2.B.3, 2.B.4, 2.B.5, 2.B.6, 2.B.8	Chemical processes	677.0
4	SETTLEMENTS	1.A.4, 1.A.5.a, 1.A.5.b.i, 1.A.5.b.ii	Energy for buildings	3322.7
5	AVIATION	1.A.3.a_CRS	Aviation cruise	412.2
		1.A.3.a_CDS	Aviation climbing & descent	305.5
		1.A.3.a_LTO	Aviation landing & take off	97.7
6	TRANSPORT	1.A.3.b	Road transportation	5530.6
		1.A.3.d	Shipping	819.1
		1.A.3.c, 1.A.3.e	Railways, pipelines, off-road transport	255.2
7	OTHER	1.A.1.b, 1.A.1.c, 1.A.5.b.iii, 1.B.1.c, 1.B.2.a.iii.4, 1.B.2.a.iii.6, 1.B.2.b.iii.3	Oil refineries and Transformation industry	1917.8
		1.B.2.a.ii, 1.B.2.a.iii.2, 1.B.2.a.iii.3, 1.B.2.b.ii, 1.B.2.b.iii.2, 1.B.2.b.iii.4, 1.B.2.b.iii.5, 1.C	Fuel exploitation	258.4
		1.B.1.a	Coal production	7.0
		3.C.2, 3.C.3, 3.C.4, 3.C.7	Agricultural soils	99.1
		2.D.3, 2.B.9, 2.E, 2.F, 2.G	Solvents and products use	168.3

To summarize, the final uncertainties per geographical entity per ECMWF fossil CO_2 emission group are based on: emission budgets calculated from CHE_EDGAR-ECMWF_2015 maps (upgraded combination of EDGARv4.3.2 and EDGARv4.3.2_FT2015), uncertainty default values from IPCC (2006) and IPCC-TFI (2019), Tier 1 approach (error propagation method) and the definition of a log-normal distribution (needed for non-negative anthropogenic CO_2 emissions). It should be noted that all uncertainty calculations were done per country (geographical entity) and only then for comparison purposes aggregated to Europe (28 members till end 2019) or global values assuming no correlation following IPCC (2006). Figure 1 shows a simplified scheme of the uncertainty calculation roadmap, followed by a detailed description below on how exactly yearly and monthly uncertainties are calculated.

https://doi.org/10.5194/essd-2020-68
Preprint. Discussion started: 6 April 2020

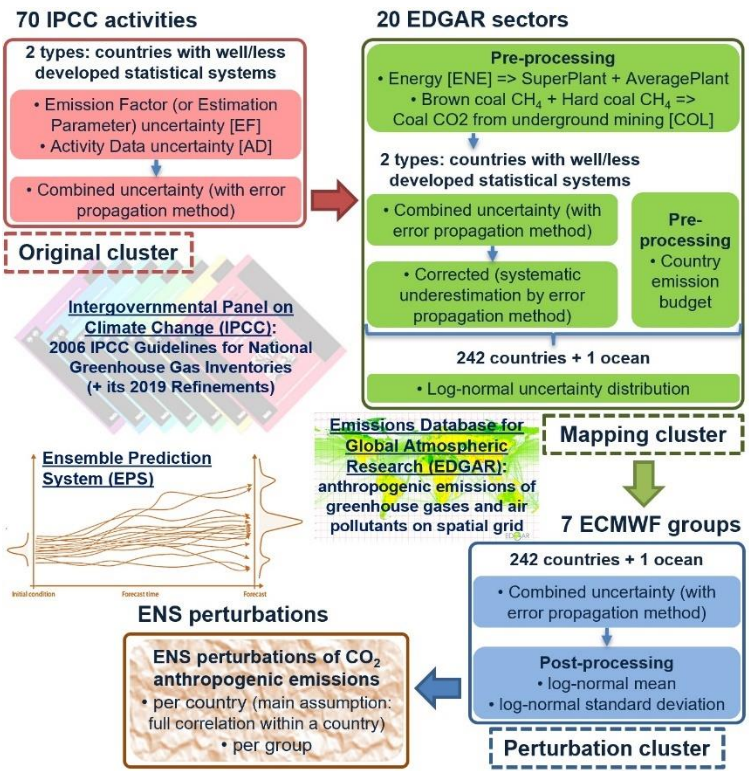

Figure 1: Simplified roadmap for yearly uncertainty calculation

3.2 Yearly uncertainties

Uncertainties in the emissions per IPCC activity from Table 2 – Combined Uncertainties UC_{IPCCi} – were calculated using uncertainties for emission factors EF_{IPCCi} and activity data AD_{IPCCi} in % provided in IPCC (2006) and IPCC-TFI (2019) following Eq. (1):

$$UC_{IPCCi} = \sqrt{EF_{IPCCi}^2 + AD_{IPCCi}^2}. \quad (1)$$

It should be noted that IPCC (2006) and IPCC-TFI (2019) provide upper and lower limits of EF and AD, which are not always symmetrical. In order to preserve as much initial information as possible (and not to inflate artificially lower or upper limits of log-normal emission distributions) all calculations were performed for upper and lower uncertainty limits separately although it is not required by the Approach 1 methodology. Moreover, IPCC (2006) provide default EF values for different fuels in transport-related activities (e.g. railways, aviation, etc.). Detailed fuel consumption information per activity was not available and it was decided to use the most typical and consumed (common) fuel type (its EF value) per each activity. The following fuels were assumed as most typical ones: for aviation – jet kerosene, for railways – diesel, and for shipping (or

https://doi.org/10.5194/essd-2020-68
Preprint. Discussion started: 6 April 2020

water-borne navigation) – composition of 80 % diesel and 20 % residual fuel oil. Following IPCC (2006) recommendations for road and off-road transport the most typical EF uncertainty was used (instead of the typical fuel type EF).

Uncertainties for each of the 70 IPCC activities from Table 2 are calculated with the error propagation method and combined into the 20 EDGAR sectors, following Eq. (2):

$$UC_{EDGARj} = \sqrt{UC_{IPCC1}^2 + UC_{IPCC2}^2 + \dots + UC_{IPCCn}^2}, \quad (2)$$

where *EDGARj* – combined uncertainty per sector *j*, and *1,2,...,n* – IPCC activities that are taken into account in a particular EDGAR sector; UC_{IPCC1}, UC_{IPCC2},..., UC_{IPCCn} used in %.

The EDGAR sector uncertainty had to be corrected, as the error propagation method of Approach 1 systematically underestimates the uncertainty unless the model is purely additive, which was not the case. Here, uncertainty calculations are estimated based on the sum of several product terms. To fix this underestimation IPCC (2006) advises using a correction factor. One example of a correction factor is proposed in Frey (2003), where the performance of an analytical approach for combining uncertainty in comparison to a Monte Carlo simulation with large sample sizes for many cases involving different ranges of uncertainty for additive, multiplicative, and quotient models are evaluated. Frey found that error propagation and Monte Carlo simulated estimates of the uncertainty half-range of the model output agreed well for values of less than 100 %, but with the increase of the uncertainty a systematic underestimation of uncertainty in the total inventory by the error propagation approach appeared. The relationship between the simulated and propagated error estimates was found to be well-behaved, which led to a correction factor development for the large (i.e. greater than 100 %) total inventory uncertainties. This correction factor will not necessarily be reliable for very large uncertainties (i.e. greater than 230 %) because it was calibrated over the range of 10 to 230 %. As such, the correction factor *FC*, calculated following Eq. (3), was applied if half-range uncertainty estimated from the error propagation method was > 100 and < 230 % following Eq. (4):

$$FC_{EDGARj} = \left[\frac{-0.7200 + 1.0921 \cdot UC_{EDGARj} - 1.63 \cdot 10^{-3} \cdot UC_{EDGARj}^2 + 1.11 \cdot 10^{-5} \cdot UC_{EDGARj}^3}{UC_{EDGARj}}\right]^2, \quad (3)$$

$$\left(UC_{EDGARj}\right)_{corr} = UC_{EDGARj} \cdot FC_{EDGARj}, \quad (4)$$

where *corr* corresponds to the corrected uncertainty; UC_{EDGARj} is given in %. In cases where UC_{EDGARj} was ≤ 100 and ≥ 230 %, FC_{EDGARj} was assumed to be equal to one.

For models that are purely additive, and for which the half range of uncertainty is less than approximately 50 %, a normal distribution is often an accurate assumption for the model output form. In this case, a symmetric probability distribution with respect to the mean can be assumed. But this is not the case for multiplicative (or mixed) models, or when the uncertainty is large for a non-negative variable such as anthropogenic CO_2 emissions. A log-normal distribution is typically an accurate assumption for the model output form, where the uncertainty range is not symmetric with respect to the mean, even though the variance for the total inventory may be correctly estimated from Approach 1. IPCC (2006) guidelines provide a practical methodology based on Frey (2003) for approximate asymmetric uncertainty range calculations based on the error propagation method. According to this methodology key characteristics of the 95 % confidence intervals are: (i)

https://doi.org/10.5194/essd-2020-68
Preprint. Discussion started: 6 April 2020

approximately symmetric for small ranges of uncertainty, and (ii) positively skewed for large ranges of uncertainty. This methodology was applied if the corrected lower half-range uncertainty estimated from error propagation method was ≥ 50 %. More details on the IPCC (2006) parametrisation of the log-normal distribution is given in the Supplementary Information, section S.3. Table 3 shows the prior uncertainty values for each EDGAR sector and two geographical entity types (i.e. well (WDS) and less well (LDS) statistically developed). These values are a combined IPCC activity uncertainty aggregated to EDGAR sectors with the error propagation method and corrected for this method's underestimation. Also, as an example, Table 3 shows aggregated to ECMWF groups uncertainties with ensured log-normal distribution for China (CHN), Europe (28 members till end 2019) and all world countries (GLB).

Table 3: Prior uncertainties (lower L and upper U bounds) per each EDGAR emission sector and two geographical entity types based on IPCC (2006) and IPCC-TFI (2019), and aggregated to the ECMWF group uncertainties for China (CHN), Europe (E28) and globe (GLB)

№	ECMWF group	IPCC (2006) activities per EDGAR sector	Prior uncertainty bounds, %				Uncertainty bounds, %					
			WDS countries		LDS countries		CHN, WDS		E28, WDS		GLB, mix	
			L	U	L	U	L	U	L	U	L	U
1	ENERGY_S	1.A.1.a (subset)	8.6	3.0	12.2	3.0	8.6	3.0	5.4	1.9	3.6	1.0
2	ENERGY_A	1.A.1.a (rest)	8.6	8.6	12.2	12.2	8.6	8.6	2.8	2.8	3.5	3.5
		4.C	40.3	40.3	41.2	41.2						
3	MANUFACTURING	1.A.2	8.6	8.6	12.2	12.2	12.8	19.4	3.9	5.8	5.7	8.6
		2.C.1, 2.C.2	37.1	37.1	37.1	37.1						
		2.C.3, 2.C.4, 2.C.5, 2.C.6, 2.C.7	73.2	73.2	73.2	73.2						
		2.D.1, 2.D.2, 2.D.4	121.7	121.7	124.0	124.0						
		2.A.1, 2.A.2, 2.A.3, 2.A.4	70.9	70.9	93.0	93.0						
		2.B.1, 2.B.2, 2.B.3, 2.B.4, 2.B.5, 2.B.6, 2.B.8	107.8	89.9	107.8	89.9						
4	SETTLEMENTS	1.A.4, 1.A.5.a, 1.A.5.b.i, 1.A.5.b.ii	12.2	12.2	26.0	26.0	12.2	12.2	4.2	4.2	3.9	3.9
5	AVIATION	1.A.3.a_CRS	5.5	6.4	50.1	106.8	3.5	4.1	1.4	1.6	17.3	58.1
		1.A.3.a_CDS	5.5	6.4	50.1	106.8						
		1.A.3.a_LTO	5.5	6.4	50.1	106.8						
6	TRANSPORT	1.A.3.b	5.4	5.4	7.1	7.1	5.1	8.2	1.6	1.8	4.3	6.4
		1.A.3.d	5.4	5.1	50.0	50.0						
		1.A.3.c, 1.A.3.e	50.3	106.9	50.5	107.0						
7	OTHER	1.A.1.b, 1.A.1.c, 1.A.5.b.iii, 1.B.1.c, 1.B.2.a.iii.4, 1.B.2.a.iii.6, 1.B.2.b.iii.3	54.4	149.3	57.7	151.4	39.7	180.9	10.1	45.3	11.5	52.4
		1.B.2.a.ii, 1.B.2.a.iii.2, 1.B.2.a.iii.3, 1.B.2.b.ii, 1.B.2.b.iii.2, 1.B.2.b.iii.4, 1.B.2.b.iii.5, 1.C	191.1	339.1	210.9	364.5						
		1.B.1.a	115.8	300.5	115.8	300.5						
		3.C.2, 3.C.3, 3.C.4, 3.C.7	70.7	0.0	70.7	0.0						
		2.D.3, 2.B.9, 2.E, 2.F, 2.G	25.0	25.0	50.0	50.0						

The next step is to combine these prior uncertainties for each EDGAR sector into ECMWF group uncertainties (see Table 3). Sector uncertainties are combined into group uncertainties by addition following Eq. (5) and Eq. (6):

https://doi.org/10.5194/essd-2020-68
Preprint. Discussion started: 6 April 2020

$$UC_{ECMWFk} = \frac{\sqrt{(\{(UC_{EDGAR1})_{corr}\}_{ln} \cdot E_{EDGAR1})^2 + (\{(UC_{EDGAR2})_{corr}\}_{ln} \cdot E_{EDGAR2})^2 + \cdots + (\{(UC_{EDGARn})_{corr}\}_{ln} \cdot E_{EDGARn})^2}}{|E_{EDGAR1} + E_{EDGAR2} + \cdots + E_{EDGARn}|}, \quad (5)$$

$$E_{ECMWFk} = E_{EDGAR1} + E_{EDGAR2} + \cdots + E_{EDGARn}, \quad (6)$$

where UC_{ECMWFk} and E_{ECMWFk} – combined uncertainty and total emissions per group *k*; *1,2,…,n* – EDGAR emission sectors that are combined in a particular ECMWF group *k*; $\{(UC_{EDGAR1})_{corr}\}_{ln}, \{(UC_{EDGAR2})_{corr}\}_{ln}, \ldots, \{(UC_{EDGARn})_{corr}\}_{ln}$ are in %. Combined group uncertainties are country-specific, because they take into account sector budget and adjust uncertainty values accordingly.

Finally, we needed to ensure a log-normal distribution of CO_2 emissions. Upper and lower uncertainty half-range values per ECMWF group *k ECMWFk* are descriptive, but not straight forward to use for emission perturbations in ensemble runs or flux inversions, where mean and standard deviation of the distribution are usually used. The lower and upper bounds of the 95 % probability range, which are the 2.5th and 97.5th percentiles respectively, calculated assuming a log-normal distribution based on a corrected estimated uncertainty half-range from an error propagation approach, are lower and upper uncertainty values. Taking this into account and using the Z-table[2] for 2.5th and 97.5th percentiles *p*, mean μ^{ln} and standard deviation σ^{ln} of log-normal distribution can be calculated following Eq. (7):

$$Z_p = \frac{ln([E_{ECMWFk}]_p) - \mu^{ln}_{ECMWFk}}{\sigma^{ln}_{ECMWFk}}, \quad (7)$$

where the following variables are known:

$$p = 2.5 \Rightarrow Z_{2.5} = -1.96,\ [E_{ECMWFk}]_{2.5} = E_{ECMWFk} \cdot \left(1 + \frac{[UC_{ECMWFk}]_{low}}{100}\right), \quad (8)$$

$$p = 97.5 \Rightarrow Z_{97.5} = 1.96,\ [E_{ECMWFk}]_{97.5} = E_{ECMWFk} \cdot \left(1 + \frac{[UC_{ECMWFk}]_{high}}{100}\right), \quad (9)$$

then simple system could be composed and solved accordingly following Eq. (10) and Eq. (11):

$$\mu^{ln}_{ECMWFk} = ln(E_{ECMWFk}) + \frac{1}{2} ln\left(1 + \frac{[UC_{ECMWFk}]_{low}}{100}\right) + \frac{1}{2} ln\left(1 + \frac{[UC_{ECMWFk}]_{high}}{100}\right), \quad (10)$$

$$\sigma^{ln}_{ECMWFk} = \frac{ln\left(1 + \frac{[UC_{ECMWFk}]_{low}}{100}\right) - ln\left(1 + \frac{[UC_{ECMWFk}]_{high}}{100}\right)}{-3.92}, \quad (11)$$

where $[UC_{ECMWFk}]_{low}$ and $[UC_{ECMWFk}]_{high}$ are in %.

3.3 Monthly uncertainties

For Earth system modelling and data assimilation purposes a sub-yearly time scale is more appropriate. Monthly profiles are available and used in air quality models and are more certain than the sub-monthly profiles. The monthly profiles used in EDGARv4.3.2 are standardised to 12 monthly shares per EDGAR sector and per region (i.e. Northern temperate zone, Equator, Southern temperate zone). They do not take into account the specificity of a single year and are not varying within a geographical entity (country). We used these global yearly and monthly emission maps for 2010 to calculate for each month

[2] The Z-table is a mathematical table for the values of the cumulative distribution function of the normal distribution.

https://doi.org/10.5194/essd-2020-68
Preprint. Discussion started: 6 April 2020

a multiplication factor per 0.1°×0.1° grid-cell of the sector-specific maps. Then multiplication factors were combined with CHE_EDGAR-ECMWF_2015 maps and monthly country- and sector-specific CO_2 emission budgets are calculated. Uncertainties for monthly budgets are obviously larger than yearly ones and instead of one standard deviation σ (Quilcaille et al, 2018) two or three standard deviations, 2σ or 3σ respectively are commonly used (Oda et al., 2018; Andres et al., 2014; Andres et al., 2011). We decided to be more analytical:

1) to use the same procedure as for annual uncertainty calculation but base it on monthly emission budgets (i.e. uncertainties for IPCC activities are combined to EDGAR sectors with error propagation method, corrected for systematic underestimation by error propagation method, and adapted to have log-normal distribution). Obtained monthly uncertainties are the same or even smaller than the yearly ones, because empirical equations applied use emission budgets, which are smaller for individual months compared to the yearly values;

2) to calculate the correlation α (an uncertainty boosting parameter) between yearly and monthly uncertainties based on an analysis of the variations over the different months following Eq. (12):

$$(E_{YEAR} \cdot UC_{YEAR})^2 = \alpha^2 \cdot ((E_{MONTH1} \cdot UC_{MONTH1})^2 + (E_{MONTH2} \cdot UC_{MONTH2})^2 + \cdots + (E_{MONTH12} \cdot UC_{MONTH12})^2), \quad (12)$$

where E and UC correspond to sectoral emission budget and uncertainty in kton and % respectively, *YEAR,MONTH1,MONTH2,…,MONTH12* – yearly and monthly (January, February, …, December) values. Eq. (12) is based on the rule for combining uncorrelated uncertainties under addition of the error propagation equation (see Eq. (5)) and assumption that each month's uncertainty should be enhanced (boosted) by the same value;

3) to multiply the prior yearly uncertainties from Table 3 by the boosting parameter (specific per country and emission sector) and use the result as monthly prior uncertainties;

4) to iterate calculation steps 1) to 3) in order to find the best boosting parameter (to have the best fit between yearly and combined 12-month uncertainties) for each country and emission sector. Once best boosting parameter was found (i.e. maximum difference between α from previous iteration and the current one over all countries and emission sectors became less than acceptable threshold) calculated monthly uncertainties per each EDGAR sector were grouped into 7 ECMWF groups and log-normal distribution of CO_2 emissions was ensured.

Figure 2 has simplified roadmaps for yearly and monthly uncertainty calculations.

3.4 Covariance matrices

The prior error covariance matrix of the emission inventory is required as an input to the inversion system. According to the IPCC (2006) all anthropogenic CO_2 emissions are assumed to be fully uncorrelated, hence the prior error correlations between grid-cell emissions from the same sector should be assumed negligible if country- and/or sector-specific information is lacking. Only by assuming full absence of correlation it is possible to calculate emission uncertainties for each geographical entity and group of sectors with rather limited globally available information. For the first implementation, ECMWF group covariance matrices per each geographical entity have the same representation – emission group is fully

https://doi.org/10.5194/essd-2020-68
Preprint. Discussion started: 6 April 2020

correlated with itself and fully uncorrelated with any other group. Table 4 shows an example for Europe (28 members till end 2019).

Table 4: Representation of ECMWF group covariance matrices, example for Europe (E28) with diagonal values being log-normal variances ·10^{-5}

E28 Group of sectors	ENERGY_S	ENERGY_A	MANUFACTURING	SETTLEMENTS	AVIATION	TRANSPORT	OTHER
ENERGY_S	26.2	0.0	0.0	0.0	0.0	0.0	0.0
ENERGY_A	0.0	2286.8	0.0	0.0	0.0	0.0	0.0
MANUFACTURING	0.0	0.0	3435.5	0.0	0.0	0.0	0.0
SETTLEMENTS	0.0	0.0	0.0	1518.3	0.0	0.0	0.0
AVIATION	0.0	0.0	0.0	0.0	0.1	0.0	0.0
TRANSPORT	0.0	0.0	0.0	0.0	0.0	473.8	0.0
OTHER	0.0	0.0	0.0	0.0	0.0	0.0	9472.5

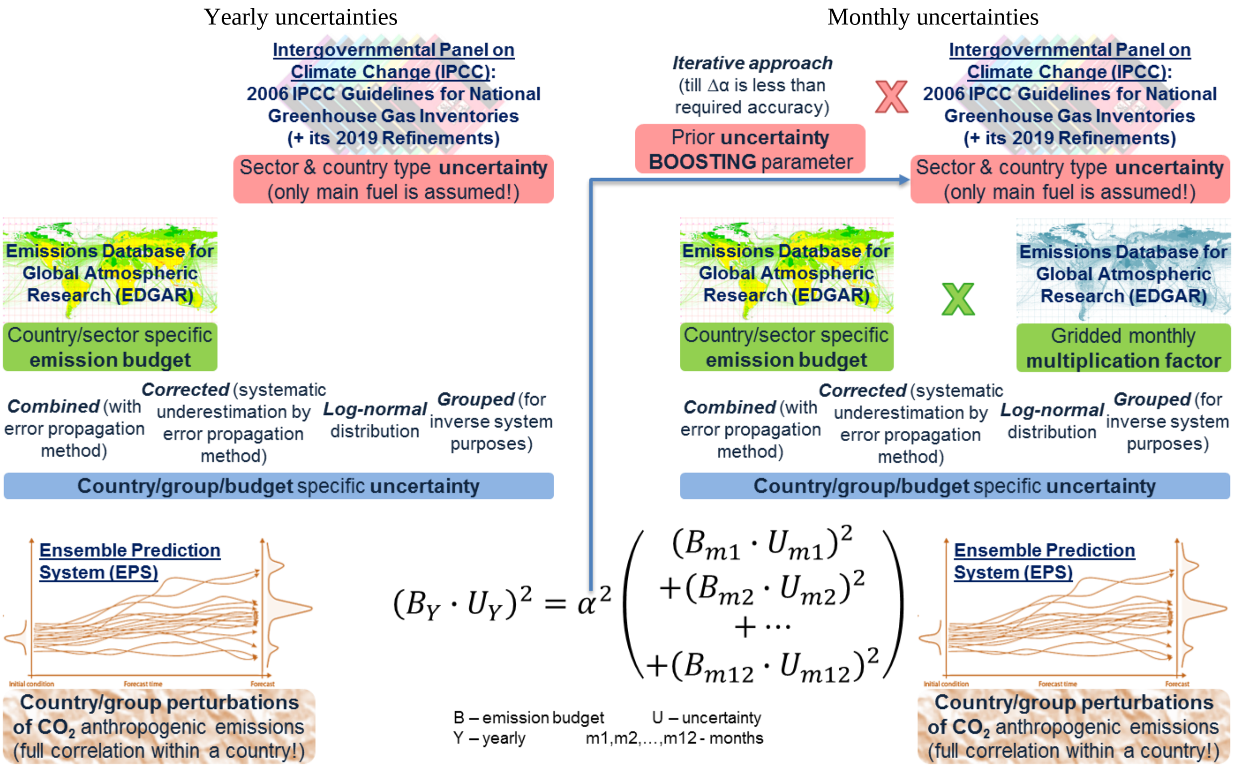

Figure 2: Simplified roadmaps for yearly (left) and monthly (right) uncertainty calculation and their relation (bottom)

https://doi.org/10.5194/essd-2020-68
Preprint. Discussion started: 6 April 2020

Open Access Earth System Science Data Discussions

Due to the lack of information available to properly characterize the error correlations and error variances in the inventory, a refinement of those prior statistics will be carried out in a follow-on paper (Busserez et al. in preparation) using atmospheric CO_2 observations. For this, the maximum likelihood of the prior error standard deviations and error correlation lengths will be estimated following approaches described in Wu et al. (2013).

4 Comparison and discussion

In this paper we decided to focus on some of the geographical areas – chosen to be among most emitting in total or per emission group, most typical or most influential for a certain region. A list of these geographical entities and development levels of their statistical infrastructures are presented in Table 5.

Table 5: List of selected geographical entities with their statistical infrastructure's development levels

ISO Code	Geographical name	Type
GLB	All World Countries	ALL
E28	Europe (28 members till end 2019)	WDS
DEU	Germany	WDS
ESP	Spain	WDS
FRA	France	WDS
GBR	United Kingdom	WDS
POL	Poland	WDS
BRA	Brazil	LDS
CHN	China	WDS
IDN	Indonesia	LDS
IND	India	WDS
JPN	Japan	WDS
RUS	Russian Federation	LDS
USA	United States of America	WDS

4.1 Global versus country-specific results

In order to see how development level of country's or geographical entity's statistical infrastructure is influencing emission uncertainty of that country or geographical entity itself and (possibly) global one, uncertainty calculations for selected entities were performed twice – with their original and inverse types (i.e. WDS becomes LDS and vice versa). More details on geographical entity's statistical infrastructure development level (e.g. how it was determined) are given in the Supplementary Information, section S.4. Figure 3 shows sectoral emission budgets, uncertainties and contributions in percentage to the total uncertainty of country or geographical entity with its original and inverse statistical infrastructure development levels. The biggest impact of development level change can be noticed for countries with larger emission budgets. On average total uncertainties of selected countries (see Table 5) changed by 1-2 %; group uncertainties changed in line with prior uncertainties from Table 3 and countries emission budgets:

- most substantial uncertainty changes for SETTLEMENTS group (consists only from residential heating emissions) with rather high differences in prior uncertainties for WDS and LDS, ±12.2 % and ±26.0 % respectively;
- strongly changes – for MANUFACTURING and ENERGY_A (and ENERGY_S where present) groups as their budgets usually make a significant part of country's total emission budget. The MANUFACTURING group is globally mainly composed from combustion for manufacturing with rather low prior uncertainty (±8.6 % and ±12.2 % for WDS and LDS respectively) and non-metallic minerals production with much higher uncertainties (±70.9 % and ±93.0 % for WDS and LDS respectively). It also contains emissions from very uncertain non-energy use of fuels (±121.7 % and ±124.0 % for WDS and LDS respectively) and chemical processes (-107.8/+89.9 % both for WDS and LDS) emissions, though their global share in this group is ~7.0 %. The ENERGY_A group is composed of emissions from average power plants with rather low uncertainties (±8.6 % and ±12.2 % for WDS and LDS respectively) and solid waste incineration with much higher uncertainties (±40.3 % and ±41.2 % for WDS and LDS respectively). For the Globe the ratio of solid waste incineration to energy emissions is ~1/100, which keeps the total ENERGY_A group prior uncertainty quite low ±3.5 % (NB! geographical entities with higher ratios will have higher uncertainties). The ENERGY_S group has emissions from super power plants only with rather low prior uncertainties (-8.6/+3.0 % and -12.2/+3.0 % for WDS and LDS respectively) for all geographical entities;
- mildly changes – for TRANSPORT group which globally is mainly composed of road transportation with rather low uncertainty (±5.4 % and ±7.1 % for WDS and LDS respectively) and shipping emissions (NB! all international shipping is included in All World Countries) with low uncertainties -5.4/+5.1 % for WDS and high uncertainties ±50.0 % for LDS countries. In addition, this group contains rather uncertain railways, pipelines and off-road transport emissions (~ -50.4/+107.0 % for both WDS and LDS), though their global share in this group is ~16.0 % only;
- small changes (though huge in % value) – for AVIATION group as its prior uncertainties change dramatically from WDS to LDS (-5.5/+6.4 % and -50.1/+106.8 % respectively), though its share in global emissions is only 2.3 % (NB! all international aviation is included in All World Countries);
- barely changes – for OTHER group as all its components are very uncertain and usually have the same prior uncertainties for both statistical infrastructure's development levels. Its main composite globally (~78.0 %) are emissions from oil refineries and transformation industry with prior uncertainties -54.4/+149.3 % and -57.7/+151.4 % for WDS and LDS respectively. Also, this group usually has the highest contribution to the geographical entity's total uncertainty.

https://doi.org/10.5194/essd-2020-68
Preprint. Discussion started: 6 April 2020

Open Access Earth System Science Data Discussions

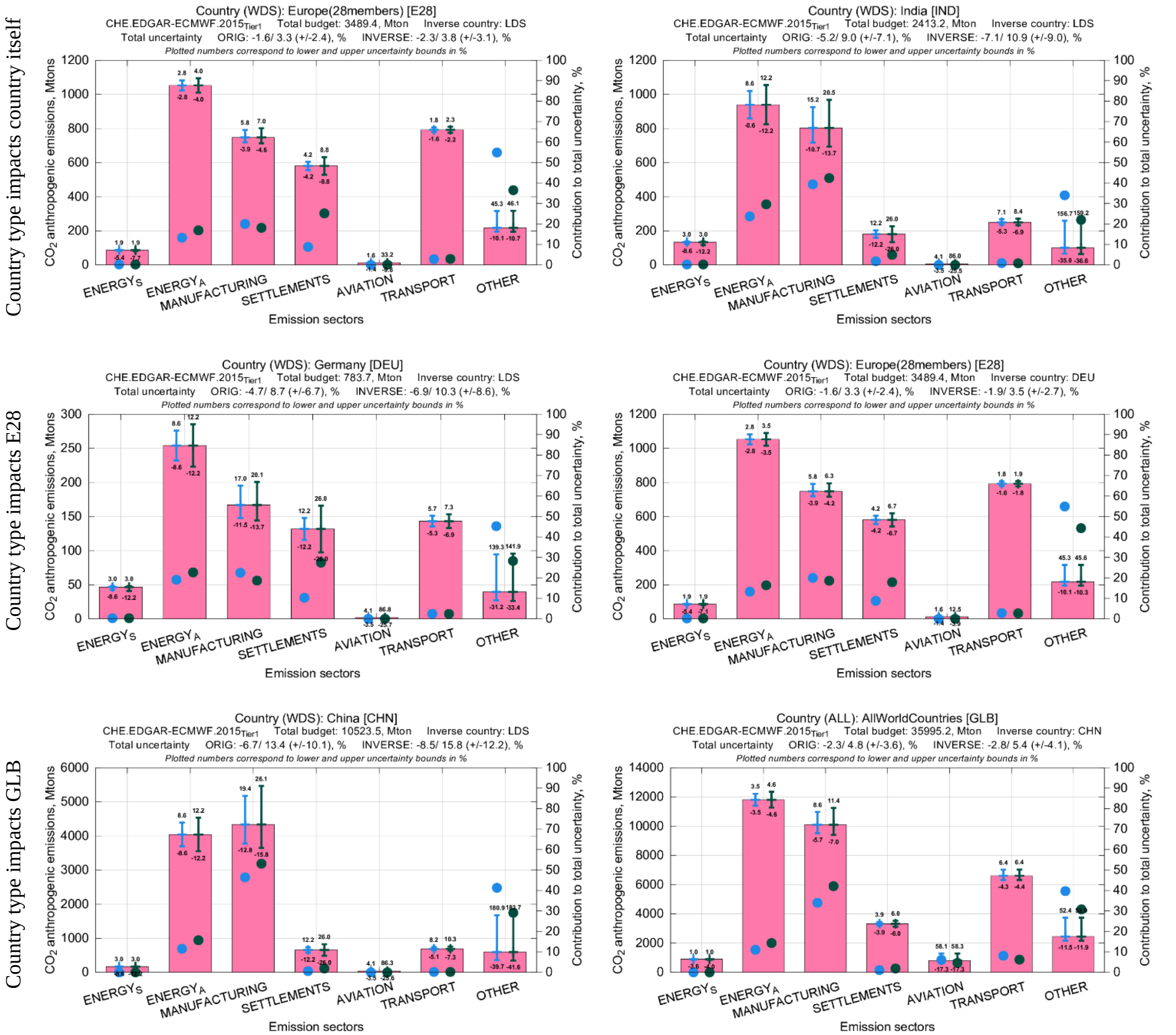

Group emission budget, in Mtons — Upper and lower group uncertainty bound for countries original and inverse type, in Mtons — Group contribution to countries total uncertainty for countries original and inverse type, in %
Group uncertainty 45.6, in %

Figure 3: Emission budgets, uncertainties and contributions in percentage to the total uncertainty of the country with their original and inverse statistical infrastructure development types: impacting mainly country itself, e.g. Europe (E28), India (IND), impacting also Europe (E28), e.g. Germany (DEU), impacting even globe (GLB), e.g. China (CHN)

Alterations in some countries' (e.g. Germany, France) statistical infrastructure's development levels lead to changes in Europe (28 members till end 2019) uncertainties, with most substantial change for SETTLEMENTS group (e.g. 2.5 and 1.0 % respectively). Huge changes (> 10.0 %) in Europe's (28 members till end 2019) AVIATION group uncertainty % value

https://doi.org/10.5194/essd-2020-68
Preprint. Discussion started: 6 April 2020

Open Access Earth System Science Data Discussions

can be due to the variation of statistical infrastructure development level for Germany, United Kingdom, France or Spain, though this groups contribution to the Europe's (28 members till end 2019) total uncertainty remains negligible. Alterations in statistical infrastructure development levels for China or United States of America modify even global uncertainties because these countries substantially contribute to the global emission budget – China emits ~1/3 of the global anthropogenic CO_2 budget and can change global total uncertainty up to 0.5 %.

4.2 Yearly and monthly uncertainties

In order to increase the emission temporal resolution, monthly emissions and their uncertainties were calculated combining yearly emissions, monthly multiplication factors, and adapted uncertainty calculation methodology (see Section 3.3). Prior yearly uncertainties were multiplied by dimensionless uncertainty boosting parameter α (same value for each month) to compute prior monthly uncertainties, which were further used together with monthly emission budgets for countries monthly uncertainty calculation. Monthly uncertainties (just like yearly uncertainties) are determined by empirical formulas from IPCC (2006), hence their values depend on monthly emission budgets, which relate to number of days in a month (e.g. even with a flat yearly cycle months with more days have higher emission budgets, i.e. month emissions are sum of daily values). To eliminate this dependency, we looked straight away at dimensionless uncertainty boosting parameter α, see Table 6 for most common values for WDS and LDS countries per EDGAR sectors. Boosting parameters become active ($\alpha \neq 1$) when absolute uncertainty values are $\geq$ 25.0 %, α increases with the increase of absolute uncertainty following third order polynomial. For lower bound uncertainties α has bigger values and steeper growth than for upper bound uncertainties (e.g. -25.0 % $\triangleq$ α = 1.5 and -124.0 % $\triangleq$ α = 2.6; +25.0 % $\triangleq$ α = 0.8 and +124.0 % $\triangleq$ α = 1.2), α behaves in the same way for WDS and LDS countries. Discrepancies in different geographical entity's (country's) boosting parameters might be for several reasons, main ones are: (i) sector emissions were zero (e.g. super power plant emissions of the energy (ENE) sector had no emissions); (ii) sector uncertainties were $\geq$ 50.0 % and needed to be adapted accordingly by log-normal distribution technique (e.g. agriculture soils (AGS) sector with prior uncertainties -70.7/+0.0 % both for WDS and LDS). Most significant discrepancies in α are for AGS sector (e.g. instead of lower/upper values from Table 6 for WDS France has α = 1.8/3.1, United Kingdom – 1.8/7.2, China – 1.8/8.4, Japan – 1.8/10.8; instead of lower/upper values from Table 6 for LDS Brazil has α = 1.8/0.0, Russian Federation – 1.8/5.6).

In general, Brazil, Indonesia and India have a very weak yearly cycle with quite high monthly uncertainties throughout the year. Globe, Europe (28 members till end 2019), Germany, Spain, France, United Kingdom, Poland, China, Japan, Russian Federation, and United States of America have more pronounced yearly cycle, most significant for SETTLEMENTS and ENERGY_A (and ENERGY_S where present) groups, and less significant for AVIATION, TRANSPORT and MANUFACTURING groups. This is in line with the monthly profiles applied in EDGARv4.3.2 for Northern and Southern temperate zones, and Equator (see Janssens-Maenhout et al. (2019)). In summer months for Northern temperate zone, a strong decrease in SETTLEMENT and ENERGY_A (and ENERGY_S where present) groups emissions was observed, a light decrease in MANUFACTURING group emissions, and a light increase in AVIATION and TRANSPORT groups

https://doi.org/10.5194/essd-2020-68
Preprint. Discussion started: 6 April 2020

Open Access Earth System Science Data Discussions

emissions. This corresponds rather well with the assumption that most of the population in the Northern hemisphere must heat their houses during winter, and that they take holidays and travel more during summer.

Table 6: Dimensionless (DN) boosting parameter uncertainties (lower L and upper U bounds) for statistically well- (WDS) and less well-developed (LDS) countries

№	ECMWF group	IPCC (2006) activities per EDGAR sector	Uncertainty boosting parameter, DN			
			WDS countries		LDS countries	
			L	U	L	U
1	ENERGY_S	1.A.1.a (subset)	1.0	1.0	1.0	1.0
2	ENERGY_A	1.A.1.a (rest)	1.0	1.0	1.0	1.0
		4.C	1.8	0.8	1.9	0.8
3	MANUFACTURING	1.A.2	1.0	1.0	1.0	1.0
		2.C.1, 2.C.2	1.7	0.8	1.7	0.8
		2.C.3, 2.C.4, 2.C.5, 2.C.6, 2.C.7	2.0	0.9	2.0	0.9
		2.D.1, 2.D.2, 2.D.4	2.6	1.2	2.6	1.2
		2.A.1, 2.A.2, 2.A.3, 2.A.4	2.0	0.9	2.3	1.0
		2.B.1, 2.B.2, 2.B.3, 2.B.4, 2.B.5, 2.B.6, 2.B.8	2.4	1.0	2.4	1.0
4	SETTLEMENTS	1.A.4, 1.A.5.a, 1.A.5.b.i, 1.A.5.b.ii	1.0	1.0	1.5	0.9
5	AVIATION	1.A.3.a_CRS	1.0	1.0	1.7	1.1
		1.A.3.a_CDS	1.0	1.0	1.7	1.1
		1.A.3.a_LTO	1.0	1.0	1.7	1.1
6	TRANSPORT	1.A.3.b	1.0	1.0	1.0	1.0
		1.A.3.d	1.0	1.0	1.7	0.9
		1.A.3.c, 1.A.3.e	1.7	1.1	1.7	1.1
7	OTHER	1.A.1.b, 1.A.1.c, 1.A.5.b.iii, 1.B.1.c, 1.B.2.a.iii.4, 1.B.2.a.iii.6, 1.B.2.b.iii.3	1.7	1.4	1.8	1.4
		1.B.2.a.ii, 1.B.2.a.iii.2, 1.B.2.a.iii.3, 1.B.2.b.ii, 1.B.2.b.iii.2, 1.B.2.b.iii.4, 1.B.2.b.iii.5, 1.C	3.0	2.4	3.1	2.5
		1.B.1.a	2.5	2.2	2.5	2.2
		3.C.2, 3.C.3, 3.C.4, 3.C.7	1.8	0.0	2.0	0.0
		2.D.3, 2.B.9, 2.E, 2.F, 2.G	1.5	0.8	1.7	0.9

4.3 Comparison with UNFCCC, TNO and other data

The CHE_EDGAR-ECMWF_2015 dataset containing 7 global gridded fossil CO_2 emission flux maps, and country- and ECMWF-group-specific emission budgets and uncertainties have been assessed with independent data. Global emission budget values from different datasets are never the same, therefore it is important to first identify why estimates differ between datasets – datasets might use same country-level information as primary input, nevertheless differences in inclusion, interpretation, and treatment of that data lead to diverse results in emissions; second – try to harmonise e.g. data inclusion or omission across datasets to have more clarity in the discrepancies.

For Europe (28 members till end 2019), Germany, Spain, France, United Kingdom, Poland, Japan, Russian Federation and United States of America emission and uncertainty data was collected from UNFCCC NIR. The aggregation of the IPCC

https://doi.org/10.5194/essd-2020-68
Preprint. Discussion started: 6 April 2020

Open Access Earth System Science Data Discussions

(2006) activity-specific emissions and uncertainties into 7 ECMWF groups was done assuming no correlation, following IPCC (2006). Although IPCC (2006) has a standard table to report GHG emissions, uncertainties can be reported in less detail by a more general category (e.g. 2.D only instead of 2.D.1, 2.D.2, 2.D.3, 2.D.4), meaning information harmonization required lots of careful time-consuming country-specific technical work.

The Netherlands Organisation for Applied Scientific Research (TNO) has recently prepared the first version of their GHG and co-emitted species emission database (TNO_GHGco_v1.1) that covers the entire European domain (at 0.1°×0.05° resolution) also for CO_2 (distinguishing between fossil fuel and biofuel). Initial emission data is from the UNFCCC (Common reporting format (CRF) tables) and the European Monitoring and Evaluation Programme/Centre on Emission Inventories and Projections for air pollutants (EMEP/CEIP). These data were harmonized, checked for gaps, errors and inconsistencies, and (where needed) replaced or completed using emission data from the Greenhouse gas-Air pollution Interactions and Synergies (GAINS) model (Amann et al., 2011). Moreover, inland shipping emissions were replaced with TNO's own estimates and sea shipping is based on automatic identification system (AIS) based tracks. Expert judgement is used to assess the quality of each data source and to make choices on which source to use. The resulting emissions were checked in detail with regard to their absolute value and trends (Kuenen et al., 2014). In this study we used emission budgets from 30 TNO sectors provided by TNO (Super et al., February 2020, personal communication), and prior uncertainties calculated from IPCC (2006) and IPCC-TFI (2019) see Table 7 (NB! all uncertainty calculations were done per country and only then for comparison purposes aggregated to Europe (28 members till end 2019) values assuming no correlation following IPCC (2006)). In addition, TNO has provided Tier 2 (Monte Carlo approach) uncertainties based on the same budgets and uncertainties from submitted NIR reports based on Tier 1 approach. The Monte Carlo simulations were done at the highest detail level (nomenclature for reporting (NFR) sector/fuel type) assuming correlations between certain sectors (for more information see Super et al. (2020)), and then emissions were aggregated to ECMWF groups assuming no correlation.

Table 7: Prior uncertainties (lower L and upper U bounds) per each TNO emission sector based on IPCC (2006) and IPCC-TFI (2019), and aggregated to the ECMWF group uncertainties for Germany (DEU) and Europe (E28)

№	ECMWF group	IPCC (2006) activities per TNO sector	Prior uncertainty bounds, %		Uncertainty bounds, %			
			WDS countries		DEU		E28	
			L	U	L	U	L	U
1	ENERGY_S	1.A.1.a (subset)	8.6	3.0	0.0	0.0	0.0	0.0
2	ENERGY_A	1.A.1.a (rest)	8.6	8.6	8.6	8.6	3.1	3.1
		4.C	40.3	40.3				
3	MANUFACTURING	1.A.2	8.6	8.6	8.3	9.0	3.0	3.6
		2.C.1, 2.C.2	37.1	37.1				
		2.C.3	10.2	10.2				
		2.C.4, 2.C.5, 2.C.6, 2.C.7	72.5	72.5				
		2.D.2	106.8	106.8				
		2.D.1, 2.D.4	50.3	50.3				
		2.A.1	36.7	36.7				

https://doi.org/10.5194/essd-2020-68
Preprint. Discussion started: 6 April 2020

		2.A.2, 2.A.3, 2.A.4	60.7	60.7				
		2.B.1, 2.B.2, 2.B.3, 2.B.4, 2.B.5, 2.B.6, 2.B.8	107.8	89.9				
4	SETTLEMENTS	1.A.4	12.2	12.2	12.1	12.1	4.2	4.2
		1.A.5.a, 1.A.5.b.i, 1.A.5.b.ii	0.0	0.0				
5	AVIATION	1.A.3.a_CRS	5.5	6.4	5.5	6.4	1.9	2.2
		1.A.3.a_CDS	5.5	6.4				
		1.A.3.a_LTO	5.5	6.4				
6	TRANSPORT	1.A.3.b	5.4	5.4	5.4	7.4	1.8	3.1
		1.A.3.d	5.4	5.1				
		1.A.3.c	5.4	5.1				
		1.A.3.e	50.0	106.7				
7	OTHER	1.A.1.b	8.6	8.6	8.1	19.6	3.7	12.4
		1.A.1.c	12.2	12.2				
		1.A.5.b.iii, 1.B.1.c, 1.B.2.a.iii.4, 1.B.2.a.iii.6, 1.B.2.b.iii.3	0.0	0.0				
		1.B.2.a.ii, 1.B.2.a.iii.2, 1.B.2.a.iii.3, 1.B.2.b.ii, 1.B.2.b.iii.2, 1.B.2.b.iii.4, 1.B.2.b.iii.5	176.3	267.2				
		1.C	50.0	100.0				
		1.B.1.a	115.8	300.5				
		3.C.2	50.0	0.0				
		3.C.3, 3.C.4, 3.C.7	50.0	0.0				
		2.D.3, 2.B.9, 2.E, 2.F, 2.G	25.0	25.0				

Figure 4 shows emission budgets and uncertainties in Mtons, and contributions in % to the total geographical entity's uncertainty for Europe (28 members till end 2019), Germany, Spain, France, United Kingdom and Poland with their original statistical infrastructure development types based on data from CHE_EDGAR-ECMWF_2015 (in pink), UNFCCC (in yellow), and TNO_GHGco_v1.1 Tier 1 (in blue) and Tier 2 (in green). Out of the four different sources, usually UNFCCC and TNO_GHGco_v1.1 Tier 2 uncertainties are the lowest ones and CHE_EDGAR-ECMWF_2015 – the highest one. It should be noted that: (i) UNFCCC uncertainties were aggregated to ECMWF groups individually per each country as uncertainties are reported in a rather free form thus could be aggregated from different levels of precision, (ii) uncertainties for Europe (28 members till end 2019) from CHE_EDGAR-ECMWF_2015 are rather low as they were calculated by aggregating information of 28 countries, rather than assuming it to be a one geographical entity from the beginning as it is done in UNFCCC, and (iii) differences in uncertainties of CHE_EDGAR-ECMWF_2015 with other sources, especially in fuel dependent emission groups, might be due to biofuels, as CHE_EDGAR-ECMWF_2015 is not taking them into account, and other sources (e.g. according to UNFCCC SETTLEMENT group uncertainties for United Kingdom are ±24.5 % (contributes 95 % of United Kingdom's total uncertainty), which is twice higher according to other sources – it might be explained by use of other fuels, e.g. wood and/or coal for residential heating). Differences in uncertainties between CHE_EDGAR-ECMWF_2015 and TNO_GHGco_v1.1 Tier 1 show additional value in more detailed emission budget knowledge, i.e. if we know for certain that country has no glass production then this rather uncertain activity can be excluded from non-metallic minerals production sector overall uncertainty calculation. Differences in uncertainties between

https://doi.org/10.5194/essd-2020-68
Preprint. Discussion started: 6 April 2020

TNO_GHGco_v1.1 Tier 1 and TNO_GHGco_v1.1 Tier 2 show additional value in advanced calculation technique, using a more sophisticated, data demanding Monte Carlo approach instead of simple error propagation. Overall there is quite good agreement in emission budgets and uncertainties from different sources of emission data.

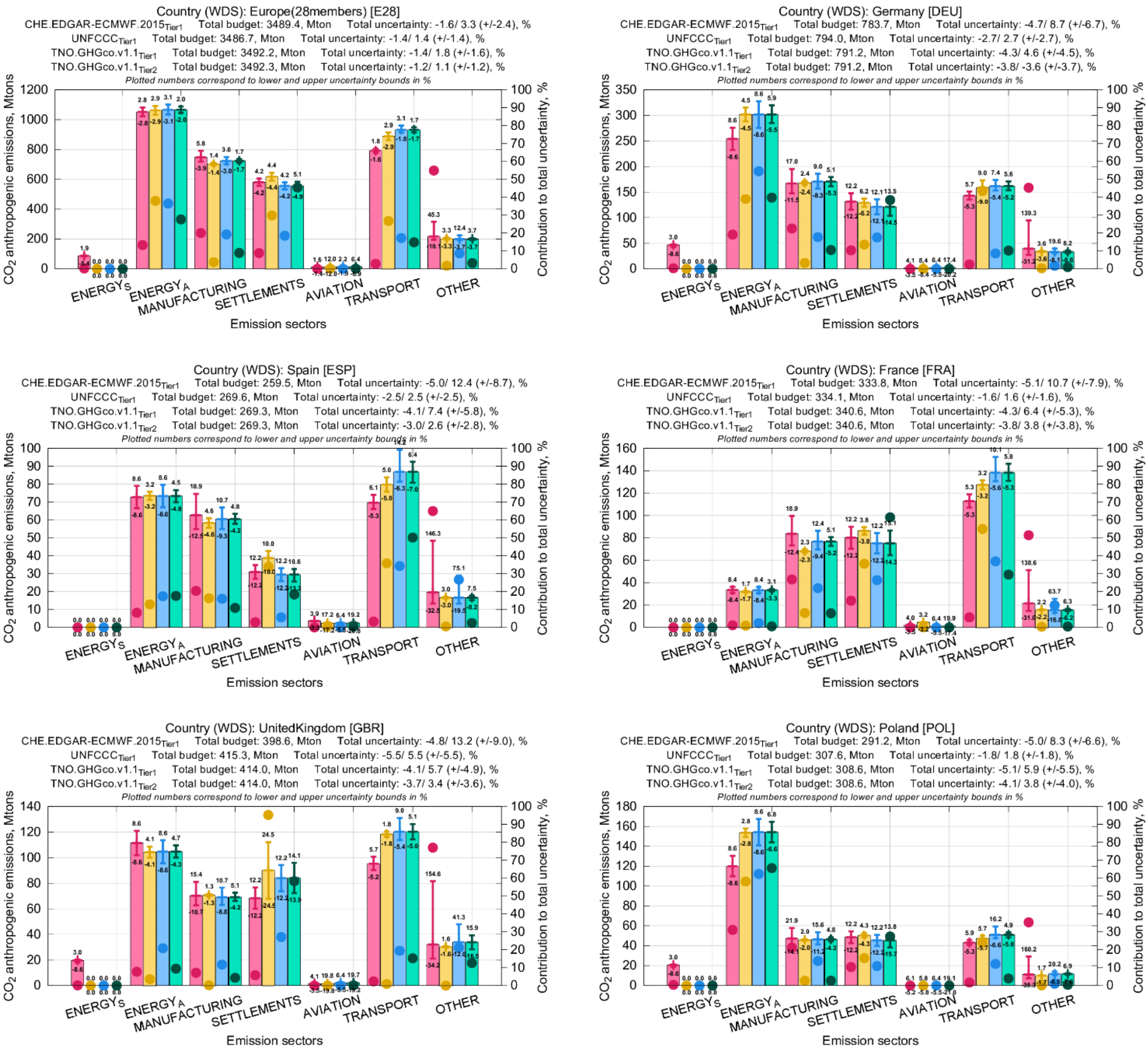

Group emission budget, in Mtons for UNFCCC, CHE_EDGAR-ECMWF_2015, TNO_GHGco_v1.1 Tier 1 & Tier 2
Group uncertainty 45.6, in %

Upper and lower group uncertainty bound, in Mtons for UNFCCC, CHE_EDGAR-ECMWF_2015, TNO_GHGco_v1.1 Tier 1 & Tier 2

Group contribution to countries total uncertainty, in % for UNFCCC, CHE_EDGAR-ECMWF_2015, TNO_GHGco_v1.1 Tier 1 & Tier 2

https://doi.org/10.5194/essd-2020-68
Preprint. Discussion started: 6 April 2020

Open Access Earth System Science Data Discussions

Figure 4: Emission budgets, uncertainties and contributions in percentage to the total uncertainty for Europe (E28), Germany (DEU), Spain (ESP), France (FRA), United Kingdom (GBR) and Poland (POL) with their original statistical infrastructure development types

Emission budgets, Tier 1 uncertainties, and contributions in percentage to the total geographical entity's uncertainty for Japan, Russian Federation and United States of America from CHE_EDGAR-ECMWF_2015 could be compared only with UNFCCC data (plots not shown here). UNFCCC uncertainties are usually lower than the ones calculated in this study. Main reason for that is use of country-specific emission data and AD uncertainties, which are lower than default values suggested by IPCC (2006) and IPCC-TFI (2019). Only for fuel dependent groups (e.g. AVIATION) UNFCCC uncertainties might be higher than in this study as rather uncertain biofuels might be taken into account. Also, emission budgets reported to UNFCCC show some differences from the ones from CHE_EDGAR-ECMWF_2015. For Japan group budgets agree rather well, and total budget difference is ~1.0 %. For Russian Federation major differences are in ENERGY_A (and ENERGY_S) and MANUFACTURING groups, which results in ~6.0 % higher total budget of CHE_EDGAR-ECMWF_2015. For United States of America major differences are ~200 Mton and ~100 Mton for SETTLEMENTS and OTHER groups respectively, which results in ~4.0 % higher total budget than based on UNFCCC data.

Recent comparison of different gridded global datasets by Andrew (2020) pointed out that only few of these datasets provide quantitative uncertainty assessment, see summary in Table 8. Comparing to other global emission uncertainty values CHE_EDGAR-ECMWF_2015 shows lowest values – it might be rather deceptive as all calculations were done at the country level and then aggregated to global level assuming no correlation following IPCC (2006), we have also calculated separately upper and lower uncertainty bounds to preserve as much initial information as possible especially of asymmetric confidence intervals for large uncertainties although it is not required by the Approach 1 methodology (according to Approach 1 from IPCC (2006) only higher uncertainty value of asymmetric interval should be used – leads to artificial inflation of uncertainty upper or lower limit); on the other hand it might be also because in this study we were not taking into account proxy grid-map uncertainties. Proxy grid-map uncertainties can be rather easily added on top of calculated uncertainties by the end user.

Table 8: Comparison of global anthropogenic CO_2 emission uncertainty at 2σ associated with certain emission dataset

Name	Global uncertainty at 2σ, %
BP	no quantitative assessment of uncertainty associated with its emissions dataset
CDIAC	±8.4 %
CEDS	no quantitative assessment of uncertainty associated with its emissions dataset, limited information in Hoesly et al. (2018)
CHE_EDGAR-ECMWF_2015	±7.1 % (-4.7/+9.6 %)
EDGAR	±9.0 %
EIA	no quantitative assessment of uncertainty associated with its emissions dataset
Global Carbon Project (GCP)	±10.0 %
IEA	no quantitative assessment of uncertainty associated with its emissions dataset

https://doi.org/10.5194/essd-2020-68
Preprint. Discussion started: 6 April 2020

Open Access Earth System Science Data Discussions

4.4 Sensitivity to the fuel specificity

As mentioned above, for transport related emission uncertainty calculations only the most typical fuel type (for aviation, railways, shipping) and EF uncertainty (for road and off-road transport) were used, because detailed fuel consumption information per IPCC activity was not available for this study. EDGAR dataset development team do have specific fuel information globally, which could be used for uncertainty calculation. EDGAR dataset with incorporated fuel-specific AD and EF uncertainties and Tier 1 approach for uncertainty calculation (see Supplementary Information, section S.5) hereinafter referred to as EDGAR-JRC. Country budget uncertainties were calculated by considering "full fuel" splitting and by taking into consideration the assumption that EF from sectors sharing the same fuel are fully correlated. This latter assumption transformed the sum in quadrature of Eq. (2) into a linear summation (Bond et al., 2004; Bergamaschi et al., 2015). The uncertainty of AD were set in accordance with IPCC (2006) guidelines, in the range 5.0 to 10.0 % for combustion activities, 10.0 to 20.0 % for combustion in the residential sector, 25.0 % for bunker fuels in the marine transport, 35.0 % for industrial processes of cement, lime, glass, ammonia (the range of uncertainty values refers to the 95 % confidence interval of the mean, assigned separately to WDS and LDS countries). Uncertainties from EDGAR-JRC dataset aggregated to the ECMWF group level were compared with the ones from CHE_EDGAR-ECMWF_2015, see Table 9 for Europe (28 members till end 2019) and all world countries (GLB), and Table S6 from the Supplementary Information, section S.5, for all the rest geographical entities from Table 5. NB! Group contribution to the geographical entity's (country's) total uncertainty is zero when group has no emissions. Emission uncertainties from EDGAR-JRC reflect the share of fuel composing the emission of each country and are in line with the estimates by CHE_EDGAR-ECMWF_2015 for those countries where the fuel-composite uncertainty is closer to the average value assigned (see Table 3). Uncertainties calculated with fuel-specific data are usually smaller; when prevailing fuel coincides with typical fuel type from CHE_EDGAR-ECMWF_2015 emission group uncertainties from both sources are quite similar. It should be noted here that: (i) countries total uncertainty is higher in EDGAR-JRC due to aggregation technique (full correlation is assumed), (ii) AVIATION group uncertainties are higher in EDGAR-JRC due to prior aggregation of all three aviation connected sectors (cruise, climbing & descent, and landing & take off).

Table 9: Aggregated to the ECMWF group level uncertainties (lower L and upper U bounds) in % and contributions in % to the total uncertainty (CV) for Europe (E28) and globe (GLB) from EDGAR-JRC (with extra fuel type knowledge) and CHE_EDGAR-ECMWF_2015 (with typical fuel only)

Country	ECMWF group	EDGAR-JRC			CHE_EDGAR-ECMWF_2015		
		L, %	U, %	CV, %	L, %	U, %	CV, %
GLB	ENERGY_S	0.0	0.0	0.0	-3.6	1.0	0.0
	ENERGY_A	-2.9	2.7	42.4	-3.5	3.5	11.0
	MANUFACTURING	-4.3	4.3	41.3	-5.7	8.6	34.0
	SETTLEMENTS	-2.5	2.5	1.9	-3.9	3.9	1.1
	AVIATION	-4.2	5.8	0.5	-17.3	58.1	6.1
	TRANSPORT	-2.5	2.6	7.7	-4.3	6.4	8.1
	OTHER	-5.9	6.2	6.2	-11.5	52.4	39.7

https://doi.org/10.5194/essd-2020-68
Preprint. Discussion started: 6 April 2020

Open Access Earth System Science Data Discussions

	TOTAL	*-4.8*	*4.8*	*100.0*	*-2.3*	*4.8*	*100.0*
E28	ENERGY_S	0.0	0.0	0.0	-5.4	1.9	0.2
	ENERGY_A	-2.0	2.4	56.4	-2.8	2.8	13.3
	MANUFACTURING	-2.2	2.2	12.6	-3.9	5.8	20.0
	SETTLEMENTS	-2.5	2.5	15.1	-4.2	4.2	8.8
	AVIATION	-2.4	2.8	0.0	-1.4	1.6	0.0
	TRANSPORT	-1.3	1.3	7.2	-1.6	1.8	2.8
	OTHER	-5.0	5.0	8.7	-10.1	45.3	54.9
	TOTAL	*-3.3*	*3.6*	*100.0*	*-1.6*	*3.3*	*100.0*

The uncertainties derived in this study are an upper bound of the uncertainty estimation compared to the uncertainties calculated with more detailed information, as done by the countries and reported to UNFCCC or to the uncertainties calculated with fuel-specific data. Even though sometimes differences might be quite high in %, they are usually quite small in Mtons. Taking into account that data is not publicly available, requires a lot of time to collect and implement, and is not available globally – it was decided not to use it in this study for Tier 1 uncertainty calculations.

4.5 Atmospheric sensitivity to nationally disaggregated emissions

The gridded emissions are a required input to the ECMWF model used to simulate atmospheric CO_2 globally (Agusti-Panareda et al., 2014; Agusti-Panareda et al., 2019). Ideally, uncertainties at a grid-cell level would be preferred by the models, which is a difficult time-consuming task. In order to check if these calculations are necessary it was decided to run some experiments. High-resolution (~25 km horizontal resolution, 137 vertical levels) simulations with ECMWF Integrated Forecasting System (IFS) model have been performed to assess the atmospheric sensitivity to fully resolved emissions compared to nationally smoothed (global emission budget is conserved), see Figure 5.

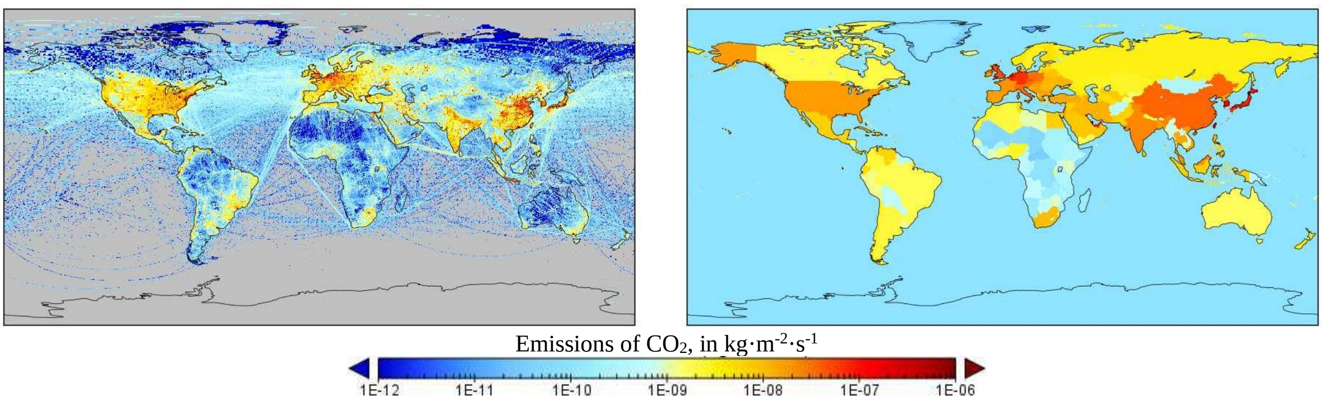

Figure 5: Anthropogenic CO_2 flux source distribution – fully resolved (left), country aggregated (right)

https://doi.org/10.5194/essd-2020-68
Preprint. Discussion started: 6 April 2020

Model simulations were performed for January 2015 with 3 hourly output. Anthropogenic, fire, ocean and biogenic fluxes (large-scale model BIAS mitigated by biogenic CO_2 flux adjustment scheme BFAS) were considered. For the full model configuration description see McNorton et al. (2020). The atmospheric response to using either fully or partially resolved emissions compared with nationally smoothed emissions after a 10-day period are shown in Figure 6. It was noted that point sources (e.g. power plants, factories) can be easily detected if they comprise substantial part of countries total emission budget (e.g. in South Africa). If point sources are distributed homogeneously over the country and other areal sources are rather high as well it becomes really difficult to detect one extra/missing emitting hotspot (e.g. in Germany). China is a very good example for both cases as its western part has very little hotspots and they are easy to detect over the low emitting background, and its eastern part has lots of hotspots and high emitting areal sources which make it almost impossible to disentangle emissions from single power plant or factory from high emitting background. In general, even by resolving a single sector, in this case the energy sector (see Figure 6), a difference in the atmospheric response is evident. Differences of several ppm are detected over multiple regions, highlighting the importance of using high resolution spatially resolved emissions. With increase of both flux and transport model resolutions these differences are expected to increase further with steeper atmospheric CO_2 gradients.

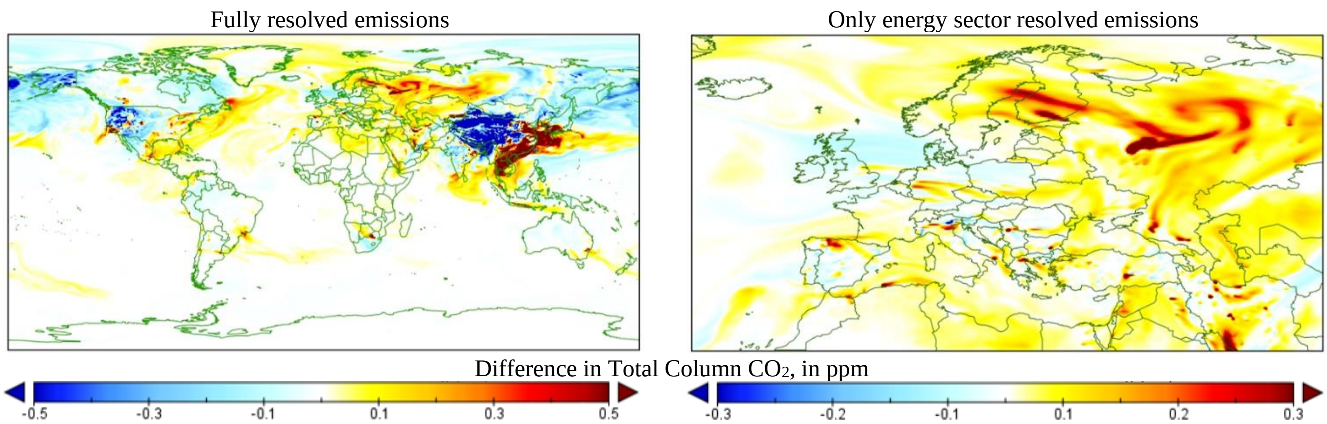

Figure 6: Difference in atmospheric response to using resolved and country aggregated emissions for January 2015 with IFS model at ~25 km resolution after 10-day simulation; the difference is calculated using both fully resolved emissions (left) or by only resolving the energy sector emissions (right)

In McNorton et al. (2020) an ensemble of the ECMWF IFS model has been used to represent the atmospheric CO_2 response to flux uncertainties derived in this study. The 50-member ensemble used spatially resolved anthropogenic, ocean, fire and biogenic fluxes. Prior anthropogenic emissions were taken from the CHE_EDGAR-ECMWF_2015 dataset and were perturbed using random noise and the log-normal yearly and monthly uncertainties reported here. They assumed that uncertainties have perfect spatial correlation within national domains and within a one-month period. No correlation was assumed between months and across different emission groups. McNorton et al. (2020) concludes that the atmospheric

https://doi.org/10.5194/essd-2020-68
Preprint. Discussion started: 6 April 2020

response to the combined anthropogenic uncertainty is between 0.1-1.4 ppm for column-averaged CO_2 over emission hot spots (see Tables 2 and 3 from McNorton et al. (2020)), these values are expected to increase further using weekly or daily uncertainty estimates. Figure 7 shows error growth in column CO_2 (XCO_2) from the ensemble simulations after 10 days using yearly and monthly uncertainties (from McNorton et al. (2020)). Results show a strong atmospheric signal from monthly uncertainties over the East Asia region, which is expected to increase further globally with hourly, daily or weekly uncertainties.

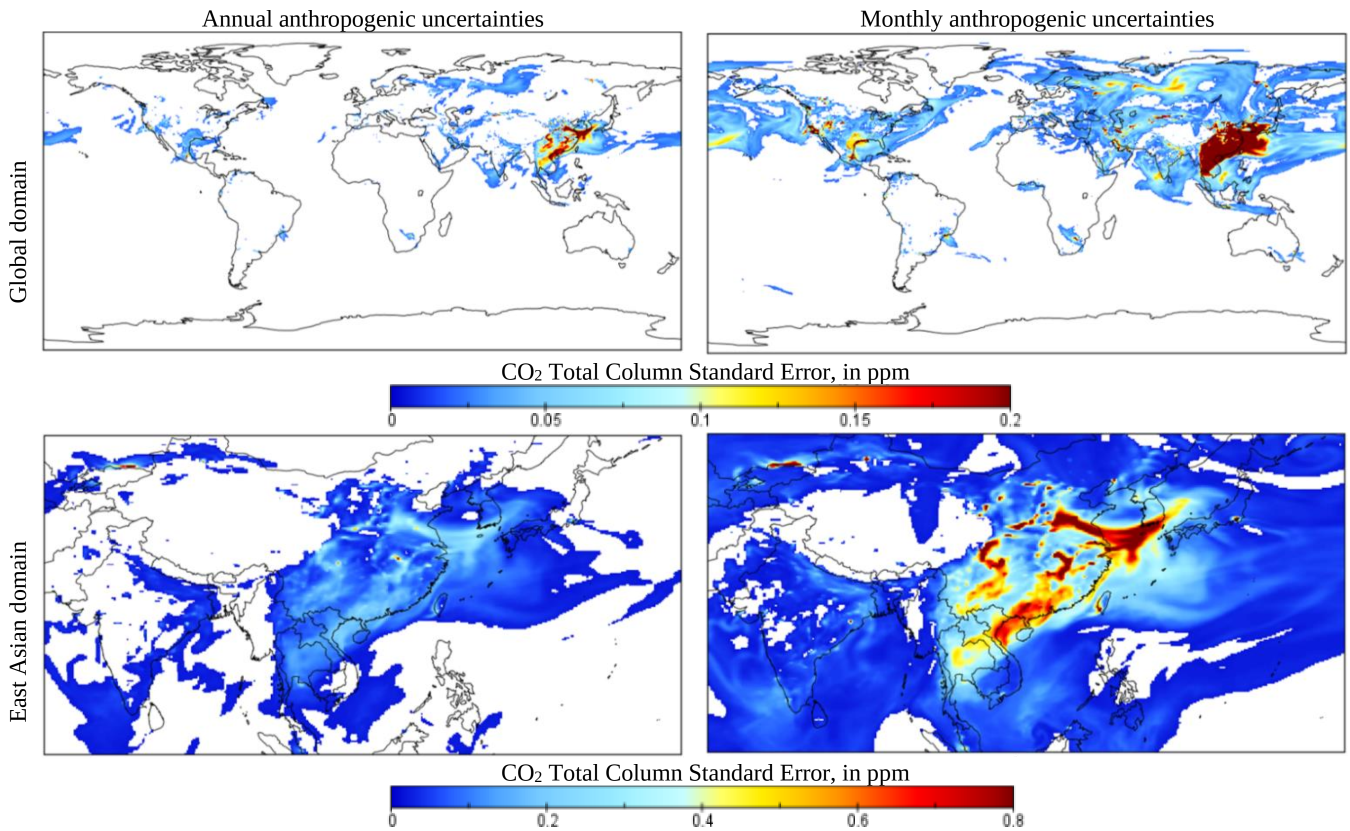

Figure 7: Error growth in column CO_2 (XCO_2) derived using IFS ensemble simulations after a 10-day period; using yearly (left) and monthly (right) uncertainties for both the global (top) and East Asian (bottom) domain

5 Conclusions

The new CHE_EDGAR-ECMWF_2015 dataset with anthropogenic fossil CO_2 emissions and their uncertainties and with a new 7×7 covariance matrix for the atmospheric transport model was compiled and tested. The fossil CO_2 emissions include all long cycle carbon emissions from human activities, such as fossil fuel combustion, industrial processes (e.g. cement) and

https://doi.org/10.5194/essd-2020-68
Preprint. Discussion started: 6 April 2020

products use, but excludes emissions from land-use change and forestry. Human CO_2 emission inventories were processed into gridded maps to provide an estimate of prior CO_2 emissions, aggregated in 7 main emissions groups: 1) power generation super-emitters and 2) energy production average-emitters, 3) manufacturing, 4) settlements, 5) aviation, 6) other transport at ground level and 7) others, with estimation of their uncertainty and covariance. For the first implementation it is assumed that each emission group is fully correlated with itself and fully uncorrelated with any other group (only diagonal values are non-zero and equal to log-normal variance). A covariance matrix of 7×7 maintains the size for the inversion system to less than 50, which is adequate and computationally affordable.

The CHE_EDGAR-ECMWF_2015 represents the 2015 fossil CO_2 emissions prior at 0.1º×0.1º resolution that has been for the first time to our knowledge completed with full uncertainty information with global coverage. Estimation of emission uncertainties is purely based on IPCC (2006) and IPCC-TFI (2019) EF and AD uncertainty values and assumptions – mainly that emissions are fully uncorrelated. Uncertainties related to the spatial distribution (representativeness of the proxy data and their uncertainty) were not assessed in this study, but they can be included by the user on top of the calculated emission uncertainties. All calculations, performed for the year 2015, are documented so that the methodology and algorithms used can be easily adapted for any other year. The dataset can be directly used in inverse modelling, and ensemble data assimilation applications, such as those envisaged within the Copernicus Atmosphere Monitoring Service (CAMS) system.

The CHE_EDGAR-ECMWF_2015 dataset consists of: (i) 1 grid-map with yearly anthropogenic CO_2 emission fluxes per each of 7 groups and 1 all groups summed together (total of 8 grid-maps), in $kg \cdot m^{-2} \cdot s^{-1}$; (ii) 2 grid-maps with yearly emissions upper and lower uncertainty bounds per each of 7 groups and 1 all groups summed together (total of 16 grid-maps), in %; (iii) 12 grid-maps with monthly anthropogenic CO_2 emission fluxes per each of 7 groups and 1 all groups summed together (total of 96 grid-maps), in $kg \cdot m^{-2} \cdot s^{-1}$; (iv) 2 grid-maps with monthly emissions upper and lower uncertainty bounds per each of 12 months and per each of 7 groups and 1 all groups summed together (total of 192 grid-maps), in %; (v) Excel file with listed information per country. The Excel file is organized in spreadsheets by: 1) geographical entities and their statistical infrastructure development levels, 2) emission groups with their prior upper and lower uncertainty bounds per each geographical entities level type and IPCC activities included in each group, 3) yearly and monthly emission budgets (per group and per geographical entity – total), uncertainties (per group and total), contribution of each group to total geographical entities uncertainty in %. For modelling purposes the CO_2 emission distribution is assumed to be log-normal with reported mean, standard deviation and variance (for the covariance matrices).

Calculated emissions and uncertainties of fossil CO_2 have been compared to other data sets based on the country-specific data reported to UNFCCC and on fuel-specific data reported in the energy statistics of IEA. The global values and their uncertainty at a 2σ range for the CHE_EDGAR-ECMWF_2015 dataset show the lowest value of -4.7/+9.6 % or ±7.1 % range (compared to CDIAC ±8.4 %, EDGAR ±9.0 %, GCP ±10.0 %), which is attributed to the methodology, in particular considering that (i) all calculations were done at the country level and then aggregated to global level assuming no correlation following IPCC (2006), and (ii) all calculations were done separately for upper and lower uncertainty bounds to preserve original information with asymmetric confidence intervals for large uncertainties (not required for the Approach 1

https://doi.org/10.5194/essd-2020-68
Preprint. Discussion started: 6 April 2020

described in IPCC (2006)), but not specified for other datasets. At country level the CHE_EDGAR-ECMWF_2015 dataset provide generally larger uncertainty ranges, that are reduced when more detailed information is available to reduce the uncertainties; in summary, using the information that is uniformly available for all countries a coherent uncertainty representation is obtained.

The CHE_EDGAR-ECMWF_2015 dataset has been tested to provide the ECMWF Earth system ensemble spread to characterise the CO_2 atmospheric concentrations' uncertainties in the prototype of the Copernicus CO_2 Monitoring and Verification Support Capacity. Annual and monthly uncertainties have been evaluated in the ECMWF's atmospheric transport model IFS ensemble simulations as well as the sensitivity to the spatial distribution of anthropogenic CO_2 emissions. Results show to be rather sensitive to the spatial distribution proxies, and most updated proxies and prior uncertainties are better adapted for data assimilation applications. This needs to be studied in a future research project, the Prototype system for a Copernicus CO_2 service (CoCO_2), that follows the current CHE research project.

Contribution of representativeness errors to uncertainties and time correlation are neglected in CHE_EDGAR-ECMWF_2015 and will need to be assessed in successive future studies. The estimation of global gridded emissions with their spatially and temporally distributed uncertainties constitute the backbone for atmospheric inversions to estimate anthropogenic emissions from atmospheric concentrations (Pinty et al., 2017). Dedicated satellite missions (e.g. Copernicus anthropogenic CO_2 monitoring mission CO_2M described in Janssens-Maenhout et al. (2020)) are being planned to monitor anthropogenic emissions from space and substantially reduce emission uncertainties. The developments in the emission uncertainty based on prior knowledge computation presented in this paper is an important preparatory step for an ensemble-based CO_2 Monitoring and Verification System prototype, such as the one developed within the CHE project.

Data availability. EDGARv4.3.2 data are open access and available at http://edgar.jrc.ec.europa.eu/overview.php?v=432&SECURE=123, last access: 26 February 2020, doi:https://data.europa.eu/doi/10.2904/JRC_DATASET_EDGAR, documented in Janssens-Maenhout et al. (2019). CHE_EDGAR-ECMWF_2015 data (Choulga et al., 2020) are freely available https://doi.org/10.5281/zenodo.3712339, and consist of following files with information on anthropogenic CO_2 emissions and their uncertainties:

- Annual_Upper_Lower_Uncertainties_Percentage_0.1_0.1.nc – file has 2×8 fields with annual upper and lower uncertainty bounds in % per each emission group and for all groups summed together on a regular grid with 1800 pixels along the latitude and 3600 pixels along the longitude, where values represent centre of the grid-cell.
  - "Lower" – lower uncertainty bound (2.5th percentile of log-normal distribution) for yearly emissions, in %;
  - "Upper" – upper uncertainty bound (97.5th percentile of log-normal distribution) for yearly emissions, in %;
  - "Sector" – emission sector numerical name. "0" represents emission group ENERGY_S (with IPCC (2006) activity 1.A.1.a (subset)) standing for power industry emissions from super emitting power plants; "1" group ENERGY_A (1.A.1.a (rest), 4.C) – power industry emissions from average emitting power plants, & solid waste incineration; "2" group MANUFACTURING (1.A.2, 2.C.1, 2.C.2, 2.C.3, 2.C.4, 2.C.5, 2.C.6, 2.C.7, 2.D.1, 2.D.2, 2.D.4, 2.A.1, 2.A.2,

https://doi.org/10.5194/essd-2020-68
Preprint. Discussion started: 6 April 2020

2.A.3, 2.A.4, 2.B.1, 2.B.2, 2.B.3, 2.B.4, 2.B.5, 2.B.6, 2.B.8) – combustion for manufacturing (including autoproducers), & iron and steel production, & non-ferrous metals production, & non energy use of fuels, & non-metallic minerals production, & chemical processes; “3” group SETTLEMENTS (1.A.4, 1.A.5.a, 1.A.5.b.i, 1.A.5.b.ii) – energy for buildings, residential heating; “4” group AVIATION (1.A.3.a_CRS, 1.A.3.a_CDS, 1.A.3.a_LTO) – aviation cruise, & climbing and descent, & landing and take off; “5” group TRANSPORT (1.A.3.b, 1.A.3.d, 1.A.3.c, 1.A.3.e) – road transportation, & shipping, & railways, pipelines, off-road transport; “6” group OTHER (1.A.1.b, 1.A.1.c, 1.A.5.b.iii, 1.B.1.c, 1.B.2.a.iii.4, 1.B.2.a.iii.6, 1.B.2.b.iii.3, 1.B.2.a.ii, 1.B.2.a.iii.2, 1.B.2.a.iii.3, 1.B.2.b.ii, 1.B.2.b.iii.2, 1.B.2.b.iii.4, 1.B.2.b.iii.5, 1.C, 1.B.1.a, 3.C.2, 3.C.3, 3.C.4, 3.C.7, 2.D.3, 2.B.9, 2.E, 2.F, 2.G) – oil refineries and transformation industry, & fuel exploitation, & coal production, & agricultural soils, & solvents and products use; “7” represents all groups summed together;

- Monthly_Upper_Lower_Uncertainties_Percentage_0.1_0.1.nc – file has 2×8×12 fields with monthly upper and lower uncertainty bounds in % per each emission group and for all groups summed together on a regular grid with 1800 pixels along the latitude and 3600 pixels along the longitude, where values represent centre of the grid-cell. File stricture is identical to the file Annual_Upper_Lower_Uncertainties_Percentage_0.1_0.1.nc, but per month (1, 2, …, 12 correspond to January, February, …, December);
- Annual_Upper_Lower_Uncertainties_0.1_0.1.nc – file has 3×8 fields with annual emissions, and upper and lower uncertainty bounds in $kg \cdot m^{-2} \cdot s^{-1}$ per each emission group and for all groups summed together on a regular grid with 1800 pixels along the latitude and 3600 pixels along the longitude, where values represent centre of the grid-cell.
  - “Sup_lower” – lower uncertainty bound (2.5^{th} percentile of log-normal distribution) for yearly emissions of ENERGY_S group, in $kg \cdot m^{-2} \cdot s^{-1}$;
  - “Sup_upper” – upper uncertainty bound (97.5^{th} percentile of log-normal distribution) for yearly emissions of ENERGY_S group, in $kg \cdot m^{-2} \cdot s^{-1}$;
  - “Sup_flux” – yearly emissions of ENERGY_S group, in $kg \cdot m^{-2} \cdot s^{-1}$;
  - “Ene_lower”, “ene_upper”, “ene_flux” – same, but for ENERGY_A group, in $kg \cdot m^{-2} \cdot s^{-1}$;
  - “Man_lower”, “man_upper”, “man_flux” – same, but for MANUFACTURING group, in $kg \cdot m^{-2} \cdot s^{-1}$;
  - “Set_lower”, “set_upper”, “set_flux” – same, but for SETTLEMENTS group, in $kg \cdot m^{-2} \cdot s^{-1}$;
  - “Avi_lower”, “avi_upper”, “avi_flux” – same, but for AVIATION group, in $kg \cdot m^{-2} \cdot s^{-1}$;
  - “Tra_lower”, “tra_upper”, “tra_flux” – same, but for TRANSPORT group, in $kg \cdot m^{-2} \cdot s^{-1}$;
  - “Oth_lower”, “oth_upper”, “oth_flux” – same, but for OTHER group, in $kg \cdot m^{-2} \cdot s^{-1}$;
  - “All_lower”, “all_upper”, “all_flux” – same, but for all groups summed together, in $kg \cdot m^{-2} \cdot s^{-1}$;
- Monthly_Sup_Upper_Lower_Uncertainties_0.1_0.1.nc – file has 3×12 fields with monthly emissions, and upper and lower uncertainty bounds in $kg \cdot m^{-2} \cdot s^{-1}$ per ENERGY_S emission group on a regular grid with 1800 pixels along the latitude and 3600 pixels along the longitude, where values represent centre of the grid-cell.

- "Sup_lower" – lower uncertainty bound (2.5th percentile of log-normal distribution) for monthly emissions of ENERGY_S group, in kg·m^{-2}·s^{-1};
- "Sup_upper" – upper uncertainty bound (97.5th percentile of log-normal distribution) for monthly emissions of ENERGY_S group, in kg·m^{-2}·s^{-1};
- "Sup_flux" – monthly emissions of ENERGY_S group, in kg·m^{-2}·s^{-1};
- "Month" – month numerical name, where 1, 2, …, 12 correspond to January, February, …, December;

- Monthly_Ene_Upper_Lower_Uncertainties_0.1_0.1.nc – file has 3×12 fields with monthly emissions, and upper and lower uncertainty bounds in kg·m^{-2}·s^{-1} per ENERGY_A emission group on a regular grid with 1800 pixels along the latitude and 3600 pixels along the longitude, where values represent centre of the grid-cell. File stricture is identical to the file Monthly_Sup_Upper_Lower_Uncertainties_0.1_0.1.nc, but with "ene_lower", "ene_upper", "ene_flux" fields;
- Monthly_Man_Upper_Lower_Uncertainties_0.1_0.1.nc – file has 3×12 fields with monthly emissions, and upper and lower uncertainty bounds in kg·m^{-2}·s^{-1} per MANUFACTURING emission group on a regular grid with 1800 pixels along the latitude and 3600 pixels along the longitude, where values represent centre of the grid-cell. File stricture is identical to the file Monthly_Sup_Upper_Lower_Uncertainties_0.1_0.1.nc, but with "man_lower", "man_upper", "man_flux" fields;
- Monthly_Set_Upper_Lower_Uncertainties_0.1_0.1.nc – file has 3×12 fields with monthly emissions, and upper and lower uncertainty bounds in kg·m^{-2}·s^{-1} per SETTLEMENTS emission group on a regular grid with 1800 pixels along the latitude and 3600 pixels along the longitude, where values represent centre of the grid-cell. File stricture is identical to the file Monthly_Sup_Upper_Lower_Uncertainties_0.1_0.1.nc, but with "set_lower", "set_upper", "set_flux" fields;
- Monthly_Avi_Upper_Lower_Uncertainties_0.1_0.1.nc – file has 3×12 fields with monthly emissions, and upper and lower uncertainty bounds in kg·m^{-2}·s^{-1} per AVIATION emission group on a regular grid with 1800 pixels along the latitude and 3600 pixels along the longitude, where values represent centre of the grid-cell. File stricture is identical to the file Monthly_Sup_Upper_Lower_Uncertainties_0.1_0.1.nc, but with "avi_lower", "avi_upper", "avi_flux" fields;
- Monthly_Tra_Upper_Lower_Uncertainties_0.1_0.1.nc – file has 3×12 fields with monthly emissions, and upper and lower uncertainty bounds in kg·m^{-2}·s^{-1} per TRANSPORT emission group on a regular grid with 1800 pixels along the latitude and 3600 pixels along the longitude, where values represent centre of the grid-cell. File stricture is identical to the file Monthly_Sup_Upper_Lower_Uncertainties_0.1_0.1.nc, but with "tra_lower", "tra_upper", "tra_flux" fields;
- Monthly_Oth_Upper_Lower_Uncertainties_0.1_0.1.nc – file has 3×12 fields with monthly emissions, and upper and lower uncertainty bounds in kg·m^{-2}·s^{-1} per OTHER emission group on a regular grid with 1800 pixels along the latitude and 3600 pixels along the longitude, where values represent centre of the grid-cell. File stricture is identical to the file Monthly_Sup_Upper_Lower_Uncertainties_0.1_0.1.nc, but with "oth_lower", "oth_upper", "oth_flux" fields;
- Monthly_All_Upper_Lower_Uncertainties_0.1_0.1.nc – file has 3×12 fields with monthly emissions, and upper and lower uncertainty bounds in kg·m^{-2}·s^{-1} for all groups summed together on a regular grid with 1800 pixels along the latitude

https://doi.org/10.5194/essd-2020-68
Preprint. Discussion started: 6 April 2020

and 3600 pixels along the longitude, where values represent centre of the grid-cell. File stricture is identical to the file Monthly_Sup_Upper_Lower_Uncertainties_0.1_0.1.nc, but with “all_lower”, “all_upper”, “all_flux” fields;

- CHE_EDGAR_2015.xlsx – file has 16 spreadsheets with listed information per country (metadata, emissions, uncertainties, statistical parameters).
  - “COUNTRY” – ISO Code (3-letter abbreviation of a geographical entity), Geographical name (name of a geographical entity), Type (development level of countries statistical system, meaning well-/less well-developed statistical system, WDS/LDS respectively), Main country (dependency, which country geographical entity in question belongs to), Full information (full name of a geographical entity, and what territory it occupies on this research map);
  - “GROUP” – № (number of anthropogenic CO_2 emission group), ECMWF group (group name), IPCC (2006) activity (IPCC activities that are included in each group), Note (short explanation of the group), Global emission budget 2015, Mton (total global emissions per group), Prior uncertainty bounds, % (initial, calculated purely based on assumptions from IPCC, lower and upper uncertainty bounds for countries with well-/less well-developed statistical systems);
  - “YEARLY” – ISO Code (3-letter abbreviation of a geographical entity), ECMWF group (group name), Budget, kton (yearly anthropogenic CO_2 emission budget per group and total per geographical entity), Uncertainty bounds, % (calculated based on Prior uncertainty bounds and Budgets yearly uncertainties per group and total per geographical entity, uncertainties lower/upper/symmetrical bounds), Contribution to total countries uncertainty, % (share of each group in geographical entities total yearly uncertainty, total contribution is always 100 %), Parameters of log-normal distribution (anthropogenic CO_2 emission distribution is assumed to be log-normal, so additionally for modelling purposes log-normal mean, log-normal standard deviation and log-normal variance were calculated);
  - “MONTHLY_01”, “MONTHLY_02”, …, “MONTHLY_12” – same explanation as for spreadsheet “YEARLY”, but for a month (01, 02, …, 12 correspond to January, February, …, December).

Author contribution. All the authors participated in the EDGAR_CHE maps generation (methodology, data generation), model experiment set-up, and analysis of the result. Margarita Choulga and Greet Janssens-Maenhout wrote the manuscript with contributions from all the other authors.

Competing interests. The authors declare that they have no conflict of interest.

Acknowledgements. The authors thank Glenn Carver (ECMWF) for editorial help and assistance; Anabel Bowen (ECMWF) for invaluable help with figure design. Margarita Choulga was funded by the CO_2 Human Emissions (CHE) project which received funding from the European Union’s Horizon 2020 research and innovation programme under grant agreement no. 776186.

https://doi.org/10.5194/essd-2020-68
Preprint. Discussion started: 6 April 2020

Financial support. This research has been supported by CHE (grant no. 776186).

References

Agustí-Panareda, A., Massart, S., Chevallier, F., Boussetta, S., Balsamo, G., Beljaars, A., Ciais, P., Deutscher, N.M., Engelen, R., Jones, L., Kivi, R., Paris, J.-D., Peuch, V.-H., Sherlock, V., Vermeulen, A.T., Wennberg, P.O., Wunch, D.: Forecasting global atmospheric CO_2, Atmos. Chem. Phys., 14, 11959-11983, doi:10.5194/acp-14-11959-2014, 2014.

Agustí-Panareda, A., Diamantakis, M., Massart, S., Chevallier, F., Muñoz-Sabater, J., Barré, J., Curcoll, R., Engelen, R., Langerock, B., Law, R.M., Loh, Z., Morguí, J.A., Parrington, M., Peuch, V.-H., Ramonet, M., Roehl, C., Vermeulen, A.T., Warneke, T., Wunch, D.: Modelling CO_2 weather – why horizontal resolution matters, Atmos. Chem. Phys., 19, 7347-7376, doi:10.5194/acp-19-7347-2019, 2019.

Amann, M., Bertok, I., Borken-Kleefeld, J., Cofala, J., Heyes, C., Höglund-Isaksson, L., Klimont, Z., Nguyen, B., Posch, M., Rafaj, P., Sandler, R., Schöpp, W., Wagner, F., Winiwarter, W.: Cost-effective control of air quality and greenhouse gases in Europe: Modelling and policy applications, Environmental Modelling and Software, Vol. 26, pp. 1489-1501, 2011.

Andres, R.J., Marland, G., Fung, I., and Matthews, E.: A 1° × 1° distribution of carbon dioxide emissions from fossil fuel consumption and cement manufacture, 1950-1990. Glob. Biogeochem. Cycles, 10, 419-429, doi:10.1029/96GB01523, 1996.

Andres, R.J., Gregg, J.S., Losey, L., Marland, G., and Boden, T. A.: Monthly, global emissions of carbon dioxide from fossil fuel consumption, Tellus B: Chemical and Physical Meteorology, 63:3, 309-327, doi:10.1111/j.1600-0889.2011.00530.x, 2011.

Andres, R.J., Boden, T.A., and Higdon, D.: A new evaluation of the uncertainty associated with CDIAC estimates of fossil fuel carbon dioxide emission, Tellus B: Chemical and Physical Meteorology, 66:1, 23616, doi: 10.3402/tellusb.v66.23616, 2014.

Andres, R.J., Boden, T.A., and Marland, G.: Annual Fossil-Fuel CO_2 Emissions: Mass of Emissions Gridded by One Degree Latitude by One Degree Longitude, United States: N. p., (NDP-058.2016), doi:10.3334/CDIAC/ffe.ndp058.2016, 2016.

Arneth, A., Sitch, S., Pongratz, J., Stocker, B., Ciais, P., Poulter, B., Bayer, A., Bondeau, A., Calle, L., Chini, L., Gasser, T., Fader, M., Friedlingstein, P., Kato, E., Li, W., Lindeskog, M., Nabel, J.E.M.S., Pugh, T.A.M., Robertson, E., Viovy, N., Yue, C., and Zaehle, S.: Historical carbon dioxide emissions caused by land-use changes are possibly larger than assumed, Nature Geoscience, 10 (2), 79, 2017.

Asefi-Najafabady, S., Rayner, P.J., Gurney, K.R., McRobert, A., Song, Y., Coltin, K., Huang, J., Elvidge, C., Baugh, K.: A multiyear, global gridded fossil fuel CO_2 emission data product: Evaluation and analysis of results, J. Geophys. Res. Atmos., 119, 17, 10.213-10.231, doi:10.1002/2013JD021296, 2014.

Bastos, A., O'Sullivan, M., Ciais, P., Makowski, D., Sitch, S., Friedlingstein, P., Chevallier, F., Rödenbeck, C., Pongratz, J., Luijkx, I.T., Patra, P.K., Peylin, P., Canadell, J.G., Lauerwald, R., Li, W., Smith, N.E., Peters, W., Goll, D.S., Jain, A.K.,

https://doi.org/10.5194/essd-2020-68
Preprint. Discussion started: 6 April 2020

Kato, E., Lienert, S., Lombardozzi, D.L., Haverd, V., Nabel, J.E.M.S., Poulter, B., Tian, H., Walker, A.P., and Zaehle, S.: Sources of Uncertainty in Regional and Global Terrestrial CO_2 Exchange Estimates, Global Biogeochemical Cycles, 34, 2, doi:10.1029/2019GB006393, 2020.

Bergamaschi, P., Corazza, M., Karstens, U., Athanassiadou, M., Thompson, R. L., Pison, I., Manning, A. J., Bousquet, P., Segers, A., Vermeulen, A. T., Janssens-Maenhout, G., Schmidt, M., Ramonet, M., Meinhardt, F., Aalto, T., Haszpra, L., Moncrieff, J., Popa, M. E., Lowry, D., Steinbacher, M., Jordan, A., O'Doherty, S., Piacentino, S., and Dlugokencky, E.: Top-down estimates of European CH4 and N2O emissions based on four different inverse models, Atmos. Chem. Phys., 15, 715–736, https://doi.org/10.5194/acp-15-715-2015, 2015.

Bond, T. C., Streets, D. G., Yarber, K. F., Nelson, S. M., Woo, J.-H., and Klimont, Z.: A technology-based Global inventory of black and organic carbon emissions from combustion, J. Geophys. Res.,109, D14203, doi:10.1029/2003JD003697, 2004.

BP: BP Statistical Review of World Energy 2016, available at: http://www.bp.com/en/global/corporate/energy-economics/statistical-review-of-world-energy.html, last access: 26 February 2020.

CarbonBrief, clear on carbon: Paris 2015: Tracking country climate pledges, available at: https://www.carbonbrief.org/paris-2015-tracking-country-climate-pledges, last access: 26 February 2020.

CHE: CO_2 Human Emissions (CHE) project official website, available at: https://www.che-project.eu, last access: 26 February 2020.

Chen, H., Huang, Y., Shen, H., Chen, Y., Ru, M., Chen, Y., Lin, N., Su, S., Zhuo, S., Zhong, Q., Wang, X., Liu, J., Li, B., Tao, S.: Modelling temporal variations in global residential energy consumption and pollutant emissions, Applied Energy, 184, 0306-2619, 820-829, doi:10.1016/j.apenergy.2015.10.185, 2016.

Choulga, M., McNorton, J., Janssens-Maenhout, G.: CHE_EDGAR-ECMWF_2015 [Data set], Zenodo, doi:10.5281/zenodo.3712339, 2020.

Cong, R., Saitō, M., Hirata, R., Ito, A., and Maksyutov, S.: Uncertainty Analysis on Global Greenhouse Gas Inventories from Anthropogenic Sources, Proceedings of the 2nd International Conference of Recent Trends in Environmental Science and Engineering (RTESE'18), Niagara Falls, Canada 10-12.06.2018, Paper No. 141, doi:10.11159/rtese18.141, 2018.

Crippa, M., Oreggioni, G., Guizzardi, D., Muntean, M., Schaaf, E., Lo Vullo, E., Solazzo, E., Monforti-Ferrario, F., Olivier, J.G.J., Vignati, E.: Fossil CO_2 and GHG emissions of all world countries - 2019 Report, EUR 29849 EN, Publications Office of the European Union, Luxembourg, ISBN 978-92-76-11100-9, doi:10.2760/687800, JRC117610, 2019.

EIA: International Energy Statistics, U.S. Energy Information Administration, Washington DC, USA, available at: https://www.eia.gov/international/overview/world, last access: 26 February 2020.

Frey, H.C.: Evaluation of an Approximate Analytical Procedure for Calculating Uncertainty in the Greenhouse Gas Version of the Multi-Scale Motor Vehicle and Equipment Emissions System, Prepared for Office of Transportation and Air Quality, U.S. Environmental Protection Agency, Ann Arbor, MI, May 30, 2003.

Friedlingstein, P., Jones, M.W., O'Sullivan, M., Andrew, R.M., Hauck, J., Peters, G.P., Peters, W., Pongratz, J., Sitch, S., Le Quere, C., Bakker, D.C.E., Canadell, J.G., Ciais, P., Jackson, R.B., Anthoni, P., Barbero, L., Bastos, A., Bastrikov, V., Becker, M., Bopp, L., Buitenhuis, E., Chandra, N., Chevallier, F., Chini, L.P., Currie, K.I., Feely, R.A., Gehlen, M., Gilfillan, D., Gkritzalis, T., Goll, D.S., Gruber, N., Gutekunst, S., Harris, I., Haverd, V., Houghton, R.A., Hurtt, G., Ilyina, T., Jain, A.K., Joetzjer, E., Kaplan, J.O., Kato, E., Klein Goldewijk, K., Korsbakken, J.I., Landschutzer, P., Lauvset, S.K., Lefevre, N., Lenton, A., Lienert, S., Lombardozzi, D., Marland, G., McGuire, P.C., Melton, J.R., Metzl, N., Munro, D.R., Nabel, J.E.M.S., Nakaoka, S.-I., Neill, C., Omar, A.M., Ono, T., Peregon, A., Pierrot, D., Poulter, B., Rehder, G., Resplandy, L., Robertson, E., Rodenbeck, C., Seferian, R., Schwinger, J., Smith, N., Tans, P.P., Tian, H., Tilbrook, B., Tubiello, F.N., van der Werf, G.R., Wiltshire, A.J., Zaehle, S.: Global Carbon Budget 2019, Earth System Science Data, 11, 4, 1783-1838, doi:10.5194/essd-11-1783-2019, 2019.

Hoesly, R.M., Smith, S.J., Feng, L., Klimont, Z., Janssens-Maenhout, G., Pitkanen, T., Seibert, J.J., Vu, L., Andres, R.J., Bolt, R.M., Bond, T.C., Dawidowski, L., Kholod, N., Kurokawa, J.I., Li, M., Liu, L., Lu, Z., Moura, M.C.P., O'Rourke, P.R., Zhang, Q.: Historical (1750-2014) anthropogenic emissions of reactive gases and aerosols from the Community Emissions Data System (CEDS), Geosci. Model Dev., 11, 369-408, doi:10.5194/gmd-11-369-2018, 2018.

IEA: Energy Balances of OECD and non-OECD countries, International Energy Agency, Paris, Beyond 2020 Online Database, available at: http://data.iea.org, last access: 26 February 2020.

IPCC: 2006 IPCC Guidelines for National Greenhouse Gas Inventories. Eggleston, S., Buendia, L., Miwa, K., Ngara, T., and Tanabe, K. (eds.). IPCC-TSU NGGIP, IGES, Hayama, Japan. www.ipcc-nggip.iges.or.jp/public/2006gl/index.html, 2006.

IPCC-TFI, Calvo Buendia, E., Guendehou, S., Limmeechokchai, B., Pipatti, R., Rojas, Y., Sturgiss, R., Tanabe, K., Wirth, T., Romano, D., Witi, J., Garg, A., Weitz, M.M., Bofeng, C., Ottinger, D.A., Dong, H., MacDonald, J.D., Ogle, S.M., Theoto Rocha, M., Sanz Sanchez, M.J., Bartram, D.M., and Towprayoon, S.: 2019 Refinement to the 2006 IPCC Guidelines for National Greenhouse Gas Inventories, Gomez, D. and Irving, W. (ed.), Vol1. Ch.8, May 2019.

Janssens-Maenhout, G., Crippa, M., Guizzardi, D., Muntean, M., Schaaf, E., Dentener, F., Bergamaschi, P., Pagliari, V., Olivier, J. G. J., Peters, J. A. H. W., van Aardenne, J. A., Monni, S., Doering, U., Petrescu, A. M. R., Solazzo, E., and Oreggioni, G. D.: EDGAR v4.3.2 Global Atlas of the three major greenhouse gas emissions for the period 1970–2012, Earth Syst. Sci. Data, 11, 959-1002, https://doi.org/10.5194/essd-11-959-2019, 2019.

Janssens-Maenhout, G., Pinty, B., Dowell, M., Zunker, H., Andersson, E., Balsamo, G., Bézy, J.-L., Brunhes, T., Bösch, H., Bojkov, B., Brunner, D., Buchwitz, M., Crisp, D., Ciais, P., Counet, P., Dee, D., Denier van der Gon, H., Dolman, H., Drinkwater, M., Dubovik, O., Engelen, R., Fehr, T., Fernandez, V., Heimann, M., Holmlund, K., Houseling, S., Husband, R., Juvyns, O., Kentarchos, A.,. Landgraf, J., Lang, R., Löscher, A., Marshall, J., Meijer, Y., Nakajima, M., Palmer, P., Peylin, P., Rayner, P., Scholze, M., Sierk, B., and Veefkind, P.: Towards an operational anthropogenic CO_2 emissions monitoring and verification support capacity, Bull. Amer. Meteor. Soc., 0, doi:10.1175/BAMS-D-19-0017.1, 2020.

Kuenen, J.J.P., Visschedijk, A.J.H., Jozwicka, M., and Denier van der Gon, H.A.C.: TNO-MACC_II emission inventory; a multi-year (2003–2009) consistent high-resolution European emission inventory for air quality modelling, Atmos. Chem. Phys., 14, 10963-10976, https://doi.org/10.5194/acp-14-10963-2014, 2014.

Le Quéré, C., Andrew, R.M., Friedlingstein, P., Sitch, S., Hauck, J., Pongratz, J., Pickers, P.A., Korsbakken, J.I., Peters, G.P., Canadell, J.G., Arneth, A., Arora, V.K., Barbero, L., Bastos, A., Bopp, L., Chevallier, F., Chini, L.P., Ciais, P., Doney, S.C., Gkritzalis, T., Goll, D.S., Harris, I., Haverd, V., Hoffman, F.M., Hoppema, M., Houghton, R.A., Hurtt, G., Ilyina, T., Jain, A.K., Johannessen, T., Jones, C.D., Kato, E., Keeling, R.F., Goldewijk, K.K., Landschutzer, P., Lefevre, N., Lienert, S., Liu, Z., Lombardozzi, D., Metzl, N., Munro, D.R., Nabel, J.E.M.S., Nakaoka, S., Neill, C., Olsen, A., Ono, T., Patra, P., Peregon, A., Peters, W., Peylin, P., Pfeil, B., Pierrot, D., Poulter, B., Rehder, G., Resplandy, L., Robertson, E., Rocher, M., Rodenbeck, C., Schuster, U., Schwinger, J., Seferian, R., Skjelvan, I., Steinhoff, T., Sutton, A., Tans, P.P., Tian, H., Tilbrook, B., Tubiello, F.N., van der Laan-Luijkx, I.T., van der Werf, G.R., Viovy, N., Walker, A.P., Wiltshire, A.J., Wright, R., Zaehle, S., and Zheng, B.: Global Carbon Budget 2018, Earth System Science Data, 10, 4, 2141-2194, doi:10.5194/essd-10-2141-2018, 2018.

Liu, Z., Guan, D., Wei, W., Davis, S.J., Ciais, P., Bai, J., Peng, S., Zhang, Q., Hubacek, K., Marland, G., Andres, R.J., Crawford-Brown, D., Lin, J., Zhao, H., Hong, C., Boden, T.A., Feng, K., Peters, G.P., Xi, F., Liu, J., Li, Y., Zhao, Y., Zeng, N., He, K.: Reduced carbon emission estimates from fossil fuel combustion and cement production in China, Nature, 524, 7565, 335-338, doi:10.1038/nature14677, 2015.

McNorton, J., Bousserez, N., Agusti-Panareda, A., Balsamo, G., Choulga, M., Dawson, A., Engelen, R., Kiping, Z., and Lang, S.: Representing Model Uncertainty for Global Atmospheric CO_2 Flux Inversions Using ECMWF-IFS-46R1, Geoscientific Model Development Discussions, 2020, 1-30, doi:10.5194/gmd-2019-314, 2020.

Mitchell, J.F.B.: Carbon dioxide review: 1982, Edited by William C.C. Oxford University Press New York 1982, 1-469, Quarterly Journal of the Royal Meteorological Society, 110, 464, 568-569, doi:10.1002/qj.49711046421, 1984.

NIR: National Inventory Submissions 2018, available at: https://unfccc.int/process-and-meetings/transparency-and-reporting/reporting-and-review-under-the-convention/greenhouse-gas-inventories-annex-i-parties/submissions/national-inventory-submissions-2018, last access: 26 February 2020.

NOAA State of the Climate Report 2018, Chapter 2 – Global Climate, Ed. Dunn, R.J.H., Stanitski, D.M., Gobron, N., and Willett, K.M. https://www.ametsoc.net/sotc2018/Chapter_02.pdf, 2019.

Oda, T. and Maksyutov, S.: A very high-resolution (1 km × 1 km) global fossil fuel CO_2 emission inventory derived using a point source database and satellite observations of night-time lights, Atmospheric Chemistry and Physics, 11, doi:10.5194/acp-11-543-2011, 2011.

Oda, T., Maksyutov, S., and Andres, R. J.: The Open-source Data Inventory for Anthropogenic CO_2, version 2016 (ODIAC2016): a global monthly fossil fuel CO_2 gridded emissions data product for tracer transport simulations and surface flux inversions, Earth Syst. Sci. Data, 10, 87-107, https://doi.org/10.5194/essd-10-87-2018, 2018.

Oda, T., Bun, R., Kinakh, V., Topylko, P., Halushchak, M., Marland, G., Lauvaux, T., Jonas, M., Maksyutov, S., Nahorski, Z., Lesiv, M., Danylo, O., and Horabik-Pyzel, J.: Errors and uncertainties in a gridded carbon dioxide emissions inventory. Mitigation and Adaptation Strategies for Global Change, Vol. 24, 6, 1007-1050, doi:10.1007/s11027-019-09877-2, 2019.

https://doi.org/10.5194/essd-2020-68
Preprint. Discussion started: 6 April 2020

ODIAC: ODIAC Fossil Fuel CO_2 Emissions Dataset, available at: http://www.nies.go.jp/doi/10.17595/20170411.001-e.html, last access: 26 February 2020.

Olivier, J.G.J. and Janssens-Maenhout, G.: CO_2 Emissions from Fuel Combustion - 2016 Edition, IEA CO_2 report 2016, Part III, Greenhouse-Gas Emissions, ISBN 978-92-64-25856-3, 2016a.

Olivier, J.G.J., Janssens-Maenhout, G., Muntean, M., and Peters, J.A.H.W: Trends in global CO_2 emissions: 2016 report, JRC 103425, https://edgar.jrc.ec.europa.eu/news_docs/jrc-2016-trends-in-global-co2-emissions-2016-report-103425.pdf, 2016b.

Paris Agreement, official website of the European Union, available at: https://ec.europa.eu/clima/policies/international/negotiations/paris_en, last access: 26 February 2020.

Paris Agreement - Status of Ratification, official website of the United Nations Framework Convention on Climate Change, available at: https://unfccc.int/process/the-paris-agreement/status-of-ratification, last access: 26 February 2020.

Pinty, B., Janssens-Maenhout, G., Dowell, M., Zunker, H., Brunhes, T., Ciais, P., Dee, D., Denier van der Gon, H., Dolman, H., Drinkwater, M., Engelen, R., Heimann, M., Holmlund, K., Husband, R., Kentarchos, A., Meijer, Y., Palmer, P., Scholze, M.: An operational anthropogenic CO_2 emissions monitoring & verification support capacity - Baseline requirements, Model components and functional architecture, European Commission Joint Research Centre, EUR 28736 EN, doi:10.2760/39384, 2017.

Quilcaille, Y., Gasser, T., Ciais, P., Lecocq, F., Janssens-Maenhout, G., and Mohr, S.: Uncertainty in projected climate change arising from uncertain fossil-fuel emission factors, Environmental Research Letters, 13, 44017, http://doi.org/10.1088/1748-9326/aab304, 2018.

Super, I., Dellaert, S.N.C., Visschedijk, A.J.H., and Denier van der Gon, H.A.C.: Uncertainty analysis of a European high-resolution emission inventory of CO_2 and CO to support inverse modelling and network design, Atmospheric Chemistry and Physics, 20, 3, 1795-1816, doi:10.5194/acp-20-1795-2020, 2020.

Wu, L., Bocquet, M., Chevallier, F., Lauvaux, T., and Davis, K.: Hyperparameter estimation for uncertainty quantification in mesoscale carbon dioxide inversions, Tellus B: Chemical and Physical Meteorology 65, no. 1: 20894, 2013.